IMPACT OF AVIATION ON CLIMATE

FAA's Aviation Climate Change Research Initiative (ACCRI) Phase II

BY GUY P. BRASSEUR, MOHAN GUPTA, BRUCE E. ANDERSON, SATHYA BALASUBRAMANIAN, STEVEN BARRETT, DAVID DUDA, GREGG FLEMING, PIERS M. FORSTER, JAN FUGLESTVEDT, ANDREW GETTELMAN, RANGASAYI N. HALTHORE, S. DANIEL JACOB, MARK Z. JACOBSON, AREZOO KHODAYARI, KUO-NAN LIOU, MARIANNE T. LUND, RICHARD C. MIAKE-LYE, PATRICK MINNIS, SETH OLSEN, JOYCE E. PENNER, RONALD PRINN, ULRICH SCHUMANN, HENRY B. SELKIRK, ANDREI SOKOLOV, NADINE UNGER, PHILIP WOLFE, HSI-WU WONG, DONALD W. WUEBBLES, BINGQI YI, PING YANG, AND CHENG ZHOU

Current and future climate impacts of aviation emissions are quantified using a combination of atmospheric models, surface and satellite observations, and laboratory experiments.

During the course of flight, aircraft burn fuel and emit gases and particles into the atmosphere, primarily at cruise altitudes within the upper troposphere and the lower stratosphere (UTLS). These emissions include carbon dioxide (CO_2), water vapor (H_2O), hydrocarbons (HC), carbon monoxide (CO), nitrogen oxides (NO_x or NO + NO_2), sulfur oxides (SO_x), and nonvolatile black carbon (BC or

AFFILIATIONS: BRASSEUR—Max Planck Institute for Meteorology, Hamburg, Germany, and National Center for Atmospheric Research, Boulder, Colorado; GUPTA, HALTHORE, AND JACOB—Federal Aviation Administration, Washington, D.C.; ANDERSON AND MINNIS—NASA Langley Research Center, Hampton, Virginia; BALASUBRAMANIAN AND FLEMING—Volpe Center, Department of Transportation, Cambridge, Massachusetts; BARRETT, PRINN, SOKOLOV, AND WOLFE—Massachusetts Institute of Technology, Cambridge, Massachusetts; DUDA—SSAI/NASA Langley Research Center, Hampton, Virginia; FORSTER—University of Leeds, Leeds, United Kingdom; FUGLESTVEDT AND LUND—CICERO, Norway; GETTELMAN—National Center for Atmospheric Research, Boulder, Colorado; JACOBSON—Stanford University, Palo Alto, California; KHODAYARI*, OLSEN, AND WUEBBLES—University of Illinois at Urbana–Champaign, Champaign, Illinois; LIOU—University of California, Los Angeles, Los Angeles, California; MIAKE-LYE AND WONG*—Aerodyne Research Inc., Billerica, Massachusetts; PENNER AND ZHOU—University of Michigan, Ann Arbor, Michigan; SCHUMANN—DLR, Munich, Germany; SELKIRK—NASA Goddard Space Flight Center, Greenbelt, Maryland; UNGER—Yale University, New Haven, Connecticut; YI AND YANG—Texas A&M University, College Station, Texas
* **CURRENT AFFILIATION:** KHODAYARI—California State University, Los Angeles, Los Angeles, California: WONG—University of Massachusetts—Lowell, Lowell, Massachusetts
CORRESPONDING AUTHOR: Guy P. Brasseur, Max Planck Institute for Meteorology, Atmosphere in the Earth System, Bundestr. 53, Hamburg 20146, Germany
E-mail: brasseur@ucar.edu

The abstract for this article can be found in this issue, following the table of contents.

DOI:10.1175/BAMS-D-13-00089.1

In final form 15 May 2015

soot). These emissions undergo complex interactions among themselves and with the changing background atmosphere.

The impact of these emissions on UTLS has been examined for several decades (Schumann 1994; Brasseur et al. 1998; Penner et al. 1999; Lee et al. 2009, hereafter LEE2009). Emissions identified as potentially affecting climate include radiatively and/or chemically active species such as CO_2, BC, NO_x, HC, CO, SO_x, and H_2O. Direct emissions of gases (e.g., CO_2, H_2O, soot particles), by-products (e.g., O_3, stratospheric H_2O), and perturbed methane (CH_4) tend to have a warming effect [positive radiative forcing (RF)].[1] Gaseous emissions of SO_x and NO_x evolve and partially transform into volatile nitrate and sulfate aerosols and those of gaseous HC emissions into semivolatile organic particles, which also contribute to climate change. Particles like sulfates generally have a cooling effect (negative RF) unless they coat soot particles, which exert warming effects. Note that BC particles are normally considered to be the main component of soot particles.

Persistent linear contrails produced in the wake of aircraft contribute to net climate warming. Contrail-induced cirrus clouds (AIC) are also expected to affect the solar and terrestrial infrared radiative budget of the atmosphere, but the corresponding radiative forcing estimates remain highly uncertain. The NO_x–O_3–CH_4 chemistry is also rather complex and leads to a direct *short-term* ozone production that produces a positive RF. The related increase in the OH radicals produces a *long-term* reduction in ambient methane (CH_4) causing a negative RF and a further long-term but small decrease in ozone causing a related negative RF (Wild et al. 2001). Also, since water vapor is an end product of CH_4 oxidation, a decrease in atmospheric CH_4 slightly decreases stratospheric water vapor. Figure 1 shows a schematic representation of the linkage between aviation emissions and their endpoint impacts through complex Earth system interactions.

There is a wide range of spatial (from plume for contrails to global domain for CH_4) and temporal (from hours for contrails and aerosols to decades for CH_4) scales associated with atmospheric perturbations due to non-CO_2 aviation emissions. The level of scientific understanding for non-CO_2 climate impacts of aviation emissions ranges from "very low" for contrail cirrus to "medium" for changes to CH_4 (IPCC 2007).

The RF metric, a backward-looking measure of the effect of emissions on the radiative flux balance, is commonly used to compare changes in climate forcings (IPCC 1990; Prather et al. 1999; Wuebbles et al. 2010). Within the aviation context, the RF for non-CO_2 aviation emissions results from processes occurring with different time scales: contrails formed in the last few hours, aerosols emitted and ozone produced from NO_x emissions in the last few days to months, and the resulting changes in CH_4 over the last few decades. The inadequacy of RF as a proper metric for global non-CO_2 aviation climate impacts is quite well known because of the associated spatiotemporal inhomogeneities (Wuebbles et al. 2007). As a result of the nonlinear interactions, the reporting of a single value as the sum of RF of various non-CO_2 components is not correct. Similarly, climate responses to different forcing mechanisms are rather distinct.

Demand for commercial aviation, in terms of available seat miles, is expected to grow at an annual rate of 2.7% over the next 20 years [Federal Aviation Administration (FAA) aerospace forecasts: www.faa.gov/about/office_org/headquarters_offices/apl/aviation_forecasts/aerospace_forecasts/2014-2034/media/FAA_Aerospace_Forecasts_FY2014-2034.pdf]. This growth in aviation will inevitably lead to an increase in aircraft combustion emissions unless emissions mitigation options are implemented.[2]

This paper summarizes results from the second phase of the Aviation Climate Change Research Initiative (ACCRI) that focused on characterizing climate impacts of non-CO_2 aviation emissions, while including important feedback processes, some of which have not been considered previously. These processes could potentially produce significant, yet

[1] Radiative forcing (RF, expressed in W m^{-2} or mW m^{-2}) is a global index for instantaneous climate forcing that quantifies the mean net radiative energy per unit time at the top of the troposphere.

[2] The Environmentally Responsible Aviation Project (ERA; www.aeronautics.nasa.gov/isrp/era/), the Advisory Council for Aviation Research and Innovation in Europe (ACARE; www.acare4europe.org/), and the Continuous Lower Emissions Energy and Noise (CLEEN; www.faa.gov/about/office_org/headquarters_offices/apl/research/aircraft_technology/cleen/) are efforts to decrease aircraft fuel burn and NO_x emissions through maturation of advanced aircraft technology and penetration into the operating fleet. The Next Generation Air Transportation System (NextGen; www.faa.gov/nextgen/) and the European Union's Single European Sky ATM Research (SESAR; ec.europa.eu/transport/modes/air/sesar/index_en.htm) projects are exploring and implementing advanced environmentally efficient operational procedures. The Commercial Aviation Alternative Fuels Initiative (CAAFI; www.caafi.org) is a community-wide effort to advance approval and accelerate the use of alternative jet fuels.

poorly quantified, climate effects. In particular, we addressed whether indirect cloud–aerosols-related effects could potentially offset some direct forcing effects. ACCRI analyses and results are based on comprehensive interactive climate models in conjunction with satellite observational and model estimates of contrail and AIC properties rather than the simpler models primarily used in previous studies.

A synthesis of the major outcomes of the ACCRI program is presented here.

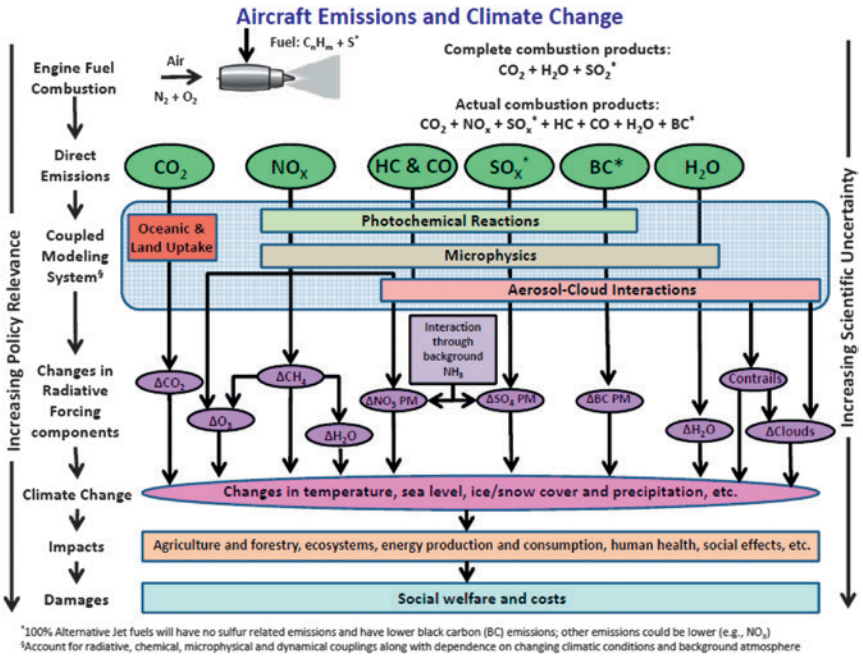

Fig. 1. Schematic representation of emissions from aircraft combustion and their potential climate and social welfare impacts. Atmospheric and climate system interactions (e.g., chemical, microphysical, dynamical, and radiative) of aircraft emissions remain poorly understood and were the focus of the ACCRI study. [Figure updated by M. Gupta (FAA) from Wuebbles et al. (2007).]

THE ACCRI PROGRAM.

The FAA started the ACCRI program in 2008 with support from the U.S. Global Climate Research Program and its participating federal agencies. Phase II of the program was established as a 3-yr activity funded by the FAA to study the potential climatic consequences of present (2006) and future (2050) commercial aviation non-CO_2 emissions, to reduce the uncertainties of those effects, and to analyze the benefits that can be derived from emissions mitigation options. Phase I of ACCRI identified key uncertainties and the need for improvement in areas of chemistry and transport processes (Toohey et al. 2010); aerosols, microphysics, and climate impacts of contrails and induced cirrus clouds (Heymsfield et al. 2010; Yang et al. 2010; Burkhardt et al. 2010); and metrics (Wuebbles et al. 2010).

Based on recommendations resulting from phase I (Brasseur and Gupta 2010), ACCRI phase II called for comprehensive research to 1) better link aviation emissions to climate impacts at global and regional scales with reduced uncertainties, 2) examine the linearity and additivity of component-based aviation-induced climate forcings and responses, 3) examine a wide spectrum of observation data from all platforms with specific attention paid to aviation emissions in flight traffic corridors, 4) investigate the impact of background atmosphere on the aviation contribution to climate change, 5) examine the impact of aviation emissions on the thermal behavior of the UTLS region, 6) examine the validity of results from simplified parametric aviation climate impact models against those derived from comprehensive models both for the present and future, and finally 7) develop contrail and induced cirrus prediction capability in regional weather models [e.g., the Weather Research and Forecasting (WRF) Model]. A synthesis of research conducted to meet these objectives with emphasis on goals 1–6 is addressed in the present paper. No study was proposed to carry out goal 7. Note that aircraft emissions also contribute to the surface air quality as a result of changes in surface ozone and particulate matter smaller than 2.5 μm ($PM_{2.5}$). However, the ACCRI program primarily focused on the contribution of full flight aviation emissions to climate change.

In particular, ACCRI called for comprehensive integrated modeling and data analysis to identify and account for atmospheric interactions and climate feedback in estimating the magnitude of non-CO_2 climate impacts and to reduce the underlying uncertainties. Other key focus areas of the ACCRI research included analysis and incorporation of results from detailed climate models into simplified models such as the Aviation Environmental Portfolio Management Tool (APMT; Mahashabde et al. 2011) and analysis of non-CO_2 climate impacts metric options such as RF, global temperature change potential (GTP),

Table 1. Project principal investigators (PIs), their affiliation, tools employed, and research description.

PI (institution)	Models, observation data, and/or laboratory techniques employed	Brief research description specific to aviation	Components of aviation atmospheric and climate impacts and interactions studied
Nadine Unger (Yale University)	GISS-E2	Multipollutant assessment of global aviation emissions impact on radiative forcing of climate in the present (2000s) and future (2050s) worlds	Ozone, methane, sulfate, nitrate, black carbon, carbon dioxide, water vapor; full treatment of oxidant–aerosol coupling; tropospheric and stratospheric chemistry
Henry Selkirk [Universities Space Research Association (USRA)/ NASA Goddard Space Flight Center (GSFC)]	GEOSCCM (free-running chemistry climate model); water vapor observations, including sondes, Measurement of Ozone and Water Vapor by Airbus In-Service (MOZAIC), and Microwave Limb Sounder (MLS) data	25-yr GEOSCCM simulations to assess impact of aviation emissions from (i) AEDT 2006 and (ii) 2050 baseline and improved technology scenarios	Impact of aviation emissions on atmospheric water vapor and ozone chemistry, particularly NO_x and HO_x
Ronald Prinn [Massachusetts Institute of Technology (MIT)]	IGSM (Sokolov et al, 2009; Prinn 2012) and APMT	Analysis of the uncertainties in climate projections using a model of intermediate complexity; application to assessing options for mitigating climate change from aviation	Impacts of emissions uncertainty, aircraft operations uncertainty, background atmospheric uncertainty, and structural model uncertainty
Donald Wuebbles [University of Illinois at Urbana–Champaign (UIUC)]	CAM4-Chem, CAM5-Chem, and climate–chemistry and Earth system climate models (Community Earth System Model, version 1.2; CESM1.2); radiative transfer model	Analyses of climate and other metrics; effects of aviation on atmospheric composition and climate through climate–chemistry modeling	Effects from aviation emissions of NO_x and other gases and particles; coupled effects from aviation emissions; metrics analyses (radiative forcing, GWPs, etc.)
Mark Z. Jacobson (Stanford University)	GATOR-GCMOM	Examination of impacts of aviation on climate and air quality with a global 3D model that treats the subgrid-scale evolution of all aircraft flights worldwide (Jacobson et al. 2011)	Effects of all aircraft emissions and specific components of aircraft emissions on global and Arctic climate, air quality, contrail formation, cirrus clouds, and atmospheric stability
Joyce Penner (University of Michigan)	CAM3+ and CAM5 GCM models coupled to the IMPACT aerosol model; limited simulations with the CAM3/IMPACT/CoCiP coupled model (Wang and Penner 2010)	Study of the effects of aircraft soot particles that have been incorporated into contrails on large-scale cirrus clouds and uncertainties associated with aerosol treatments	Impact of aerosols from contrails on large-scale clouds and radiative forcing
Andrew Gettelman (NCAR)	NCAR CESM; global climate model	Analysis of the effects of aviation water vapor and aerosols on natural cirrus clouds and contrails	Water vapor, contrails, cirrus clouds, aerosol indirect effects, and cloud life cycle

Table 1. Continued.

PI (institution)	Models, observation data, and/or laboratory techniques employed	Brief research description specific to aviation	Components of aviation atmospheric and climate impacts and interactions studied
Ping Yang (Texas A&M University)	Collocated MODIS and Cloud–Aerosol Lidar with Orthogonal Polarization (CALIOP)/*CALIPSO* observations; Rapid Radiative Transfer Model for GCMs [RRTM(G)] for SW–LW radiative transfer simulations; CAM5; the Fu–Liou radiative transfer model	Study of persistent contrails with satellite observations, contrail particle shape and optical properties, contrail radiative property parameterization for climate models, and soot-contaminated contrail cirrus and its radiative effects	Contrail geographical, geometrical, meteorological, and optical properties; a new contrail radiative property parameterization scheme; estimation of the global contrail radiative forcing; assessment of the impacts of BC on contrail optical properties
Patrick Minnis [NASA Langley Research Center (LaRC)]	*Aqua* and *Terra* MODIS data; Fu–Liou radiative transfer model; air traffic waypoints; Modern-Era Retrospective Analysis for Research and Applications (MERRA) reanalysis data; CoCiP; ECHAM4 with a contrail cirrus module (CCMod)	Determination of global linear contrail coverage and retrieval of their properties; computation of linear contrail RF; estimation of RF of spreading contrails	LC and contrail cirrus radiative impacts on climate
Hsi-Wu Wong (Aerodyne)	NASA's PAL chamber facility; Aerodyne's microphysical parcel model	Investigation of the parametric effects on contrail ice particle formation in the jet regime	Parametric effects on contrail ice particle properties such as size, composition, and concentration

regional temperature potential (RTP), and global warming potential (GWP). Refer to sidebar on "Metrics for Aviation Effects on Climate: ACCRI Contributions" for more discussion.

ACCRI relied on the multimodel and multiteam approach for model–model and model–data intercomparison of common data sources and assumptions among the studies to identify areas of agreement as well as discrepancies in the results. In addition, ACCRI invited contributions from the U.S. and international communities. These key aspects positioned ACCRI to uniquely contribute to advance the science and to better inform decision-making on technology advancement, systemwide operational improvement, and policy measures. Phase II of ACCRI included 10 funded project teams comprising 47 team members from 23 institutions worldwide. In particular, the ACCRI consortium employed several atmospheric and climate models; a range of observation datasets for meteorological, chemical, and contrails analysis; and laboratory measurements for early phase microphysical studies. Table 1 provides a summary of ACCRI phase II models, data, and laboratory techniques.

AVIATION EMISSION INVENTORIES. Worldwide inventories of full flight (LTO + non-LTO, where LTO represents the landing and takeoff cycle) aviation fuel burn and emissions were created using the FAA Aviation Environmental Design Tool (AEDT; Roof et al. 2007; see also ICAO 2013). These datasets, computed by the Department of Transportation's (DOT) Volpe Center for ACCRI 2006 and 2050 climate impacts studies, include emissions of NO_x, HC, CO, CO_2, water vapor, organic aerosols, and BC. At the engine exit plane, all emissions are gaseous except for BC. Both SO_x and HC quickly condense to form sulfate and OC aerosols. In the absence of high space–time resolution microphysical models with a capability to evolve and transform gaseous emissions into aerosols within the engine vicinity, pseudoemission rates for sulfates and OC aerosols in terms of fuel burn and fuel sulfur content (for sulfate aerosols) were employed (Barrett

et al. 2010). Gaseous emissions of SO_x are scaled from fuel burn, assuming a fuel sulfur content of 600 mg kg^{-1} fuel burn. A speciation profile (EPA–FAA 2009) is prescribed to distribute HC emissions into individual species.

For the year 2006, AEDT processed 31.3 million flights on a chorded basis for fuel burn and emissions. These chorded emissions were also gridded with a resolution of 1° × 1° in latitude and longitude and 500 ft in height. Individual research teams reconfigured these chorded and/or gridded emissions data as per their study requirements while ensuring consistency in the absolute amount, distribution, and unit conversion. Three emissions scenarios for 2050 were used. They correspond to 1) a "2050 baseline" scenario, which assumes a technology freeze with no operational improvements—that is, improvements are limited to those associated with a fleet refresh resulting from retirement and introduction of currently in-production aircraft (as of 2006) (ICAO 2013); 2) a "2050 S1" scenario built upon the baseline scenario while assuming a 2% increase in fuel efficiency per year through 2050, consistent with the ICAO aspirational goal of annual improvement in fuel efficiency, due to aircraft technology and operational improvements accompanied by a technology-driven progressive reduction in NO_x emissions (to 67% in 2016, to 47% in 2026, to 33% in 2036, and to 20% in 2050) consistent with National Aeronautics and Space Administration (NASA) N + 3 and N + 4 technology program goals and projections for fleet penetration; and 3) a "2050-S2" scenario that builds upon the 2050-S1 scenario and assumes the use of alternative jet fuel with zero sulfur emissions and 50% reduction in overall BC emissions.

The total mass of fuel burned by commercial aviation in 2006 globally is calculated to be about 188 Tg (1 Tg = 10^{12} g) (Wilkerson et al. 2010; Olsen et al. 2013a). The resulting global emissions were approximately 594 Tg for CO_2, 232 Tg for H_2O, 0.812 Tg for NO_x as N, 0.676 Tg for CO, and 9.8 10^7 kg for nonmethane HCs reported in methane mass units. Table 2 summarizes 2006 and 2050 emissions strengths for all species along with the number of flight operations and the fuel burn. Note that fuel burn and NO_x emissions for the 2050-S1 and 2050-S2 scenarios are the same because of the underlying assumptions as stated earlier.

Of particular interest are the 2005 fuel burn values used by LEE2009, which are 19% higher than those used here for the year 2006. In LEE2009, military and general aviation emissions were included. The ACCRI emissions inventory does not include contributions from these sources that explain most of the 19% difference between the two datasets.[3] We will attempt to compare ACCRI climate impacts results with those from LEE2009, wherever appropriate, while recognizing these differences.

All ACCRI models used the same background emissions of chemical species for the appropriate year based on the Intergovernmental Panel on Climate Change (IPCC) representative concentration pathway scenario (RCP4.5; van Vuuren et al. 2011).

ESTIMATES OF CLIMATE IMPACTS FOR 2006.

Aviation chemical impacts. Aircraft emissions of nitrogen oxides and other chemically reactive species affect the budget of ozone, specifically in the vicinity of the tropopause, and therefore indirectly contribute to the radiative forcing. Seven models were used in the ACCRI program to assess the effects of the 2006 aviation emissions on atmospheric ozone and related chemistry. See Table 1 for more details.

Figure 2 shows that the largest impact of aviation NO_x emissions (Olsen et al. 2013b) occurs at cruise altitude in the main flight corridors of the midlatitude Northern Hemisphere. Peak NO_x perturbations are generally around 0.07 ppb and range from 0.01 ppb [the Gas, Aerosol, Transport, Radiation, General Circulation, Mesoscale, and Ocean Model (GATOR-GCMOM)] to 0.11 ppb [NASA's Goddard Institute for Space Studies Model E2 (GISS-E2)]. In all models except one (GISS-E2), the peak absolute ozone concentration increase occurs at 10–12 km and ranges from 5 to 8 ppb (1%–7%). In the GISS-E2 results, there is a decrease in the ozone concentration above ~10 km with a minimum at 12 km. This specific behavior is probably associated with the high background (on aviation) NO_x concentration produced by this particular model and with the resulting titration of ozone by injected aviation NO_x. All models saw an increase in OH at cruise altitude (not shown here). At high NO_x, HO_2 decreases with increasing OH because of its faster reaction with NO_x; at low NO_x, HO_2 increases with increasing OH. GATOR-GCMOM predicted low NO_x as a result of more conversion of NO_x to nitrated gases and aerosols and thus an increase in HO_2 with

[3] The 2005 and 2006 aircraft emissions used by LEE2009 and ACCRI, respectively, were derived using two different emissions modeling tools as well as fleet distribution and operational activities that differed between the two. Although this is expected to be a small source of difference based on comparisons of the two approaches, it could introduce another degree of variation into the global emissions distributions and their impacts on atmospheric composition and climate impacts (Skowron et al. 2013).

Table 2. Aircraft emissions for years 2006 and 2050 (different scenarios) generated using the FAA AEDT tool. Data on fuel burned and CO_2 emissions from LEE2009 are also given for comparison.

Year	Unit	ACCRI -2006	ACCRI-2050 2050-Base	ACCRI-2050 2050-S1	ACCRI-2050 2050-S2	2005 (LEE2009)
No. of flights		31,258,625	120,994,648	120,994,648	120,994,648	*
Fuel burn	Tg	188.1	902.8	514.4	514.4	232.4
NO_x	Tg N yr^{-1}	0.812	3.950	1.570	1.570	
SO_2	Tg SO_2 yr^{-1}	0.221	1.060	0.604	0.000	
Sulfate	Gg yr^{-1}	6.780	32.510	18.520	0.000	
BC	Gg yr^{-1}	5.960	29.040	16.560	8.300	
OC	Gg yr^{-1}	6.620	27.520	15.750	15.750	
CO	Tg yr^{-1}	0.676	2.500	1.420	1.420	
Alkenes	Gg yr^{-1}	2.698	5.900	3.350	3.350	
Paraffin	Gg yr^{-1}	1.437	3.150	1.780	1.780	
CO_2	Tg yr^{-1}	594.0	2,852.0	1,625.0	1,625.0	733.0
H_2O	Tg yr^{-1}	232.0	1,111.0	633.0	633.0	

* Includes military flights and general aviation in addition to commercial flights.

increasing OH. Other models predicted a decrease in HO_2 because of predicted higher NO_x as a result of less conversion to other gases or aerosol particle components.

Global tropospheric ozone burdens for background ozone range from about 275 Tg for Integrated Global System Modeling framework (IGSM; Sokolov et al. 2009; Prinn 2012) to 373 Tg for the Community Atmosphere Model, version 4 (CAM4), simulations (Table 3). These values are within the range of model results reported in Stevenson et al. (2006) but not all model (CAM4, IGSM, GATOR-GCMOM) values are within the reported standard deviation. Changes in the tropospheric ozone mass burden due to AEDT 2006 aviation NO_x emissions range from 2.3 (GISS-E2) to 9.1 Tg [the chemical transport model (CTM) driven by the Goddard Earth Observing System Model (GEOS-Chem)], while the relative changes range from a 0.7% (GISS-E2) to 2.5% (GEOS-Chem).

Overall, the seven models show large differences in the calculated species composition due to aviation emissions, a part of which is due to differences in their simulated background atmosphere. The offline CTM model results as a group (e.g., CAM4, CAM5, GEOS-Chem), with fixed prescribed meteorology, tend to be similar in their responses and sensitivities. Models coupled at varying degrees of complexity [GISS-E2, Goddard Chemistry Climate Model (GEOSCCM), and GATOR-GCMOM] respond quite differently from each other for NO_x and O_3. Differences in the vertical resolution; details of the implementation of chemistry, aerosol, and cloud coupling processes; stratospheric chemistry–radiation interaction treatment; and differences in their background atmospheres also contribute to the differences in simulated aviation chemical impacts. Background NO_x concentrations affect the O_3 production efficiency of aviation NO_x emissions and HO_x speciation.

The range of radiative forcing due to the response of ozone to NO_x emissions in 2006 is estimated to range from 6 (for GISS-E2) to 36.5 (CAM5) mW m^{-2}. The ozone response to aircraft NO_x emissions occurs rapidly in the atmosphere and is, therefore, qualified as a "short term" ozone response. It also leads to an increase in the local concentration of hydroxyl radical concentration, which produces a small "long term" reduction in the atmospheric methane concentration and, hence, a range of reductions in radiative forcing is estimated to be from –12.3 (GEOSCCM) to –8.0 (GISS-E2) mW m^{-2}. Oxidation of the reduced amount of methane further leads to a decrease in long-term ozone (or O_3 long) and water vapor. Only one model (CAM5) attempted to

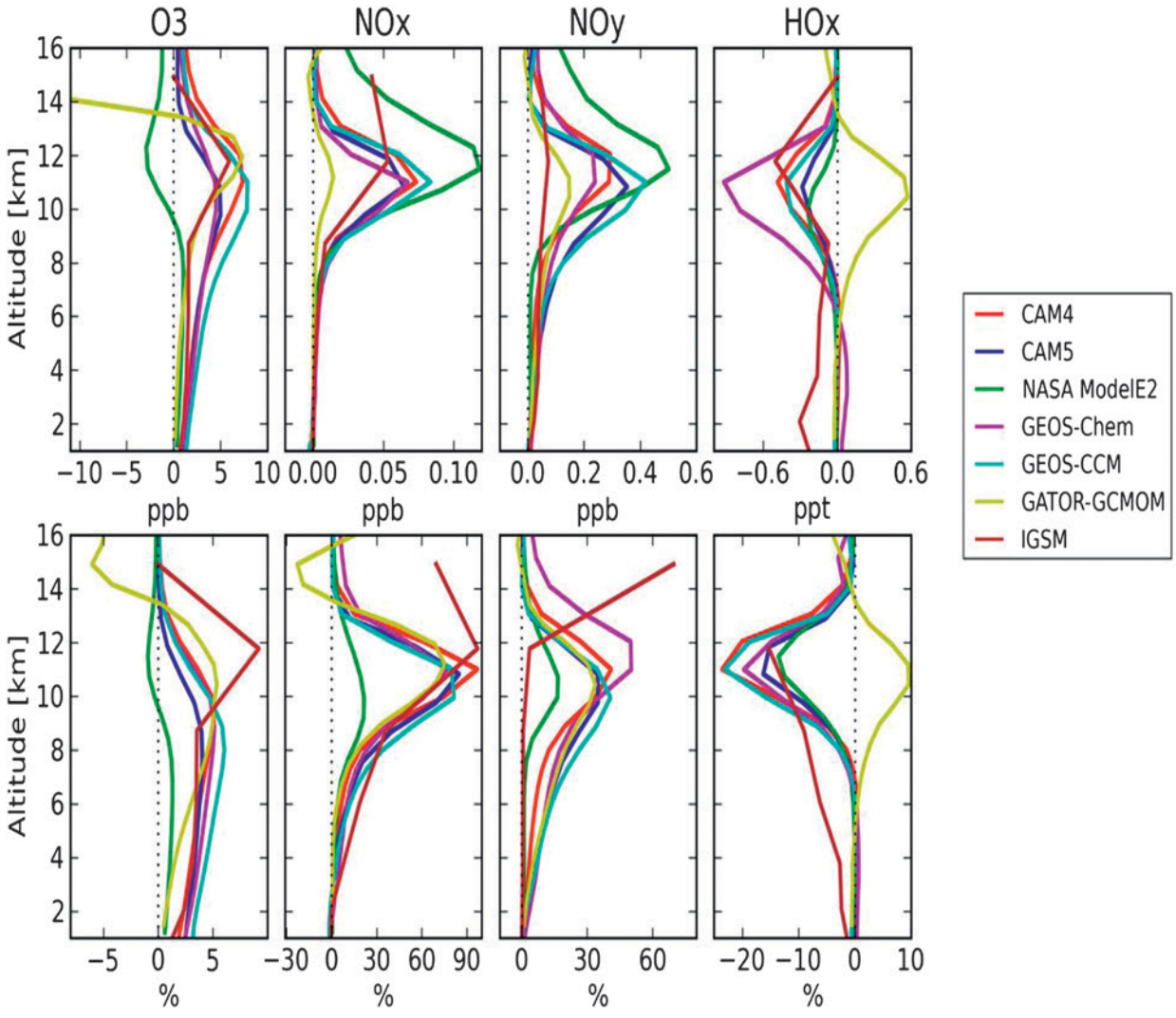

Fig. 2. Effect of aviation emissions on O_3, NO_x, NO_y, and HO_x. Profiles are zonal means averaged over 40°–60°N. (top) Absolute perturbation and (bottom) percent perturbation at each level are relative to the nonaviation background concentration at that level. Perturbations are for the AEDT 2006 aviation emissions and show that there is still a relatively large range among model estimates of the effects of aviation on atmospheric chemistry. See text for a description of the models. [Adapted from Olsen et al. (2013b).]

Table 4. Comparison of aviation emissions component-specific RF (mW m^{-2}) for the 2006 and 2050 baseline and mitigation scenarios.

Scenario	Fuel burn (Tg)	NO_x (Tg N)	O_3-S				CH_4	
			GISS-E2	IGSM	GEOSC-CM	UIUC CAM5	GISS-E2	IGSM
2006 baseline	188.1	0.812	6	26	30.5	36.5	−8	−9.7
2050 baseline	902.8	3.950	30	136	162.3	143	−35.5	−58.6
2050-S1	514.4	1.570	14	63	62.7	70.5	−15	−33.3
2050-S2	514.4	1.570	14	63			−15.5	−33.3

quantify the reduction in RF for long-term ozone and water vapor, with values of −4.5 and −2.6 mW m^{-2}, respectively (Khodayari et al. 2014). See Table 4 (and Table 7 later) for more details.

It is probably important to note that the changes in the concentrations of chemical species reported here have been derived by global chemical transport models, whose spatial resolution is too low to fully capture the details of plume shearing, stretching, and dilution in the wake of aircraft. The assumption that chemical species are well mixed within a model grid cell is a source of error that can be substantial since, in the nearly turbulence-free environment of the upper troposphere and lower stratosphere, plumes with high concentrations of effluents may persist over a relatively long time.

Table 3. Tropospheric ozone mass burdens for the 2006 background atmosphere (in Tg) and changes due to aviation emissions [in Tg (% of total)].

	2006	
Model used	**Background**	**Aviation**
UIUC CAM4	373	7.3 (2.0)
IGSM	275	4.5 (1.6)
GISS-E2	350	2.3 (0.7)
UIUC CAM5	318	5.4 (1.7)
GEOSCCM	327	6 (1.8)
GEOS-Chem	363	9.1 (2.5)
GATOR-GCMOM	280	2.5 (2.3)

Direct effects of aviation aerosols. ACCRI research studies are aimed at improving our understanding of the direct (scattering and absorption) and indirect (through altering cloud particles) effects of aerosols on the atmospheric radiation budget and climate. Aircraft combustion directly emits BC (or soot) particles. Measurements show that aircraft emit ~10^{15} soot particles (or 0.01–0.2 g soot) per kilogram of fuel burned (Penner et al. 1999). The ACCRI team used cruise-level emissions of 0.03 g BC kg^{-1} fuel with a similar amount of organic matter emitted. Number density emission indices of 2×10^{14} particles per kilogram of fuel below 3000 ft (914.4 m) and 4×10^{14} above 3000 ft were used. Within the exhaust plume these soot particles coagulate to form soot aggregates of larger sizes (10–100 nm). Two ACCRI teams (GISS-E2 and CAM5) reported direct RF due to BC aerosols in the range of 0.6 (GISS-E2) to 1.0 (CAM5) mW m^{-2} (see Table 6).

Gaseous emissions of HCs partially condense in the vicinity of the engine exit plane and form OC particles. In addition, gaseous emissions of SO_x and NO_x partially undergo chemical and physical transformation to form secondary sulfate and nitrate aerosols. Calculations performed with the CAM5 climate model suggest that aircraft SO_2 direct radiative forcing is about −3 mW m^{-2} (Gettelman and Chen 2013). In GISS-E2 the effects of aviation emissions on global radiative forcing by sulfate (−7 ± 2 mW m^{-2}) and nitrate (−4.0 ± 1 mW m^{-2}) aerosols are small but statistically significant (Unger et al. 2013). The aviation sulfate direct radiative forcing is larger than previous estimates because GISS-E2 accounts for additional oxidation of nonaviation SO_2 to sulfate via aviation NO_x effects on atmospheric oxidation capacity. The IGSM model reported RF values of −4.4 mW m^{-2} for sulfate aerosols and −7.5 mW m^{-2} for nitrate aerosols (see Table 7). Besides the models' capability to properly simulate the oxidation of gaseous emissions and the formation of particles, as well as their vertical transport and atmospheric removal, differences in assumed ammonia emissions strength and distribution in these two studies could have contributed to the differences in the reported values.

Table 4. Continued.

	CH_4		SO_4 direct		Long-term O_3	Water vapor	BC
Scenario	**GEOSCCM**	**UIUC CAM5**	**GISS-E2**	**IGSM**	**UIUC CAM5**	**UIUC CAM5**	**IGSM**
2006 baseline	−12.3	−12.3	−7	−4.4	−4.5	−2.6	0.3
2050 baseline	−72.1	−59.7	−30	−25.3	−20.3	−12.5	0.8
2050-S1	−35.5	−28.3	−17	−13	−9.4	−5.9	0.6
2050-S2			−2	−9.2			0.3

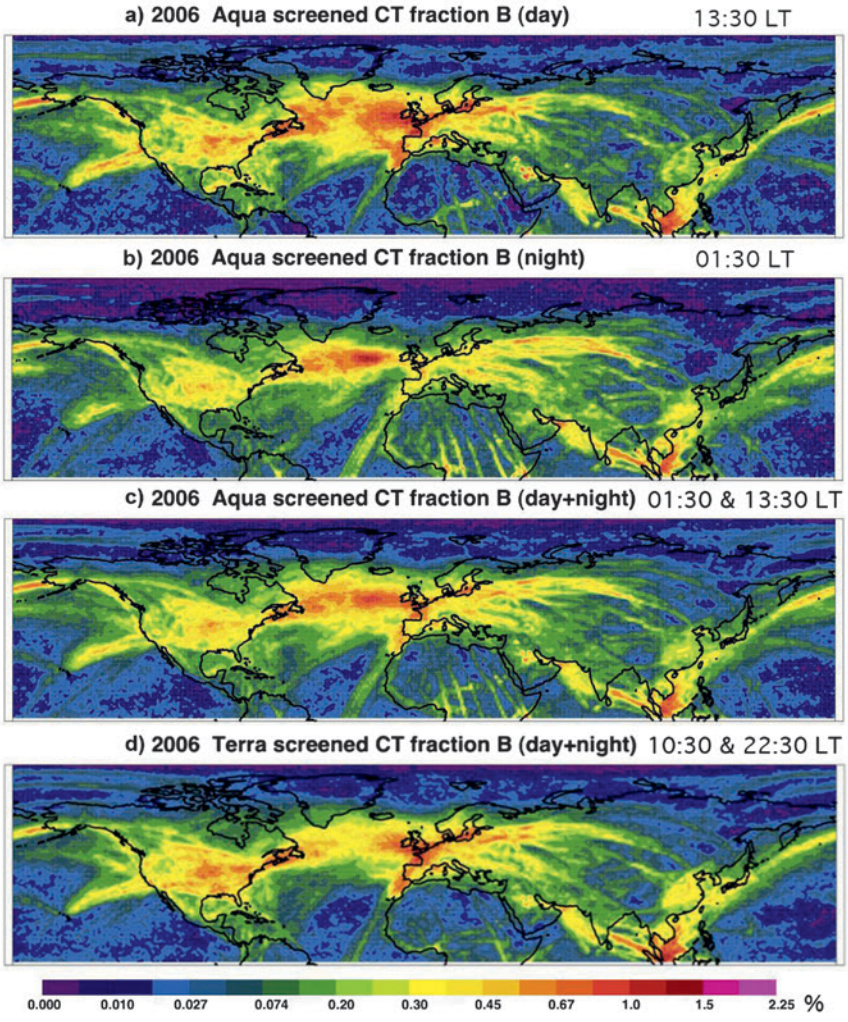

Fig. 3. Mean flight-track-screened contrail coverage fraction (%) determined using mask B of Duda et al. (2013).

Linear contrails. Linear contrails (LCs) form along an aircraft flight path when the mixture of exhaust and ambient air satisfies particular humidity and temperature conditions (Schumann 1996). Some linear contrails spread for a few hours but maintain their linear shape, enabling their detection in satellite imagery. Others spread farther, forming contrail cirrus clouds that are indistinguishable from natural cirrus. The ACCRI studies covered the full range of contrail processes from ice crystal formation near the engine exhaust to the development of contrail-induced cirrus (AICs).

The climate radiative effects of contrails are determined by the background radiation field and the contrail coverage, lifetime, temperature (T_{con}), contrail optical depth (COD), contrail particle shape, and ice crystal effective diameter (D_E). Accurate representation of observations of these parameters is necessary for model parameterization and validation and for determining contrail RF. Prior estimates of these parameters have come from various regional satellite or brief aircraft studies that yield a wide range of results with large uncertainties (e.g., Burkhardt et al. 2011; Yang et al. 2010). To reduce the uncertainties, contrail formation, persistence, and the effects on solar and thermal radiation, and therefore on climate, were investigated using a combination of laboratory experiments, observations, and climate models.

Laboratory studies. Wong et al. (2013) investigated the impact of exhaust emissions on contrail formation by introducing exhaust species into the NASA Particle Aerosol Laboratory (PAL) chamber facility. Specifically, the effects of ambient conditions, water and soot emissions, ice nuclei properties, and fuel compositions on ice particle formation were examined, particularly close to the exhaust in the jet regime (<5 s of plume age). The results were consistent with field measurements (Busen and Schumann 1995; Schumann et al. 1996, 2002) demonstrating that the formation of contrail ice particles can be reproduced in a laboratory setting. The experiments were used to validate predictions from the Aerodyne microphysical parcel model (Wong and Miake-Lye 2010) and from the large-eddy simulations (LESs) that provide early plume properties to the GATOR-GCMOM model (Naiman et al. 2011).

In addition to the nominal conditions representing current fleet emissions, Wong et al. (2013) also explored scenarios representing future fleet burning alternative fuels, such as low-soot emissions and zero- to low-sulfur emissions. These parameters have never been studied in in situ measurements since it is currently not possible to burn zero-sulfur or zero-aromatic fuels in a jet engine. Wong et al. (2013) found that hydrophilic uptake on soot, achieved by sulfate emissions or certain organic emissions, is necessary

for the formation of contrail ice particles. The soot surface with reduced hydrophilicity also induced an increased humidity threshold for ice formation. These experimental results suggest that the formation of ice particles with zero-sulfur or low-soot emissions may be drastically different and that the emissions inventory values representing future fleet burning alternative fuels may need to be further revised to give more accurate predictions of the contrail radiative forcing.

ACCRI researchers also examined the relationships between contrail ice particles and soot emissions. Wong et al. (2013) identified internal mixing of soot in ice particles as being dominant in comparison to external mixing. To understand the effect of internal and external mixing of soot with ice particles on the contrail radiative properties, Liou et al. (2011, 2013) used the geometric-optics surface-wave (GOS) approach, which represents the contrail ice crystals by a simple hexagonal plate model. They found a large enough forcing to cause the cloud heating rate to increase by from 0.3 to 1.4 K day^{-1} in the internally mixed case compared to the pure ice case. This can lead to a reduction of atmospheric heating below the cloud. However, Hong and Minnis (2015) showed that embedded ammonium sulfate particles and air bubbles reduce the asymmetry factor and increase the extinction efficiency of small ice crystals at solar wavelengths. Thus, these types of inclusions would increase the reflectivity of contrails—an effect that could offset some of the soot-induced increase in contrail RF.

Observational studies. For the first time, the ACCRI program, using satellite data, characterized near-global linear contrail coverage and its optical and radiative properties (T_{con}, D_E, and COD) and the corresponding RF. Duda et al. (2013) developed an optimized linear contrail detection algorithm (CDA) for application to Moderate Resolution Imaging Spectroradiometer data (MODIS; Barnes et al. 1998) and produced the most comprehensive LC observational dataset to date (Fig. 3) by analyzing all Northern Hemisphere MODIS data during 2006. Their best estimate of mean hemispheric LC coverage of 0.135% yields a 0.07% global average when extrapolated to the Southern Hemisphere. This estimate is less than the 0.087% global estimate from Bakan et al. (1994), who extrapolated visual analyses of northeast Atlantic Advanced Very High Resolution Radiometer (AVHRR) data to the global scale and is within the range of 0.06%–0.15% simulated by GATOR-GCMOM. The *Aqua* afternoon contrail coverage (Fig. 3a) peaks at 1.2% over several oceanic air routes. Just after midnight (Fig. 3b), LC coverage is less everywhere except over a few areas, including the mid–North Atlantic, where it is 1.25%. The combined day and night *Terra* results (Fig. 3d) differ spatially from *Aqua* (Fig. 3c) because the corresponding air traffic patterns change between the respective overpass times, yielding more contrails over the United States and northern Europe, where air traffic density is greatest. The relatively small coverage over the United States and Europe, particularly in the *Aqua* results, is at least partially due to the frequent occurrence of overlapped contrails and greater background radiance variability over land than over water.

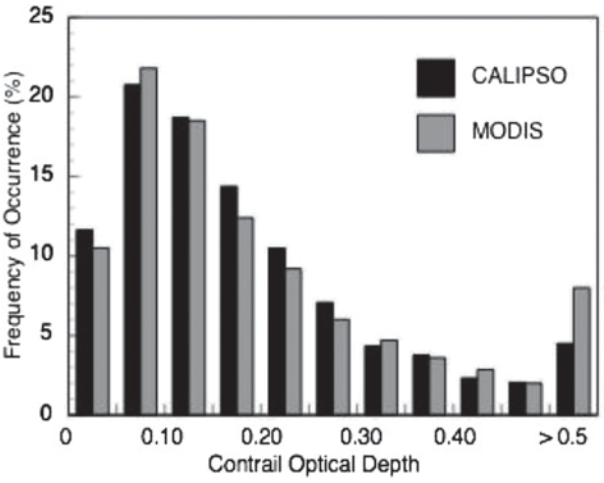

Fig. 4. Probability distributions of CODs derived from 2009 *CALIPSO* data (Iwabuchi et al. 2012) and *Aqua* MODIS data (Bedka et al. 2013).

Two approaches were used to assess contrail properties. Iwabuchi et al. (2012) analyzed collocated MODIS and *Cloud–Aerosol Lidar and Infrared Pathfinder Satellite Observations* (*CALIPSO*; Winker et al. 2007) lidar data corresponding to several thousand LCs detected visually in MODIS imagery. They found that the LC temperatures averaged −54.6° ± 5.3°C with a mean COD of 0.19 from off-nadir *CALIPSO* data. From the lidar backscatter, they concluded that a compact crystal with D_E of approximately 20 μm is a reasonable choice as a typical ice crystal model for contrails. In addition, they provided unprecedented statistics on contrail length, width, and depth for detailed contrail model validation. Xie et al. (2012) also employed collocated MODIS and *CALIPSO* LC observations to develop a contrail particle habit (shape) parameterization that best matched the observed lidar parameters. These parameterizations are already advancing the capabilities for modeling of contrails and their impacts on climate (Schumann 2012; Schumann and Graf 2013).

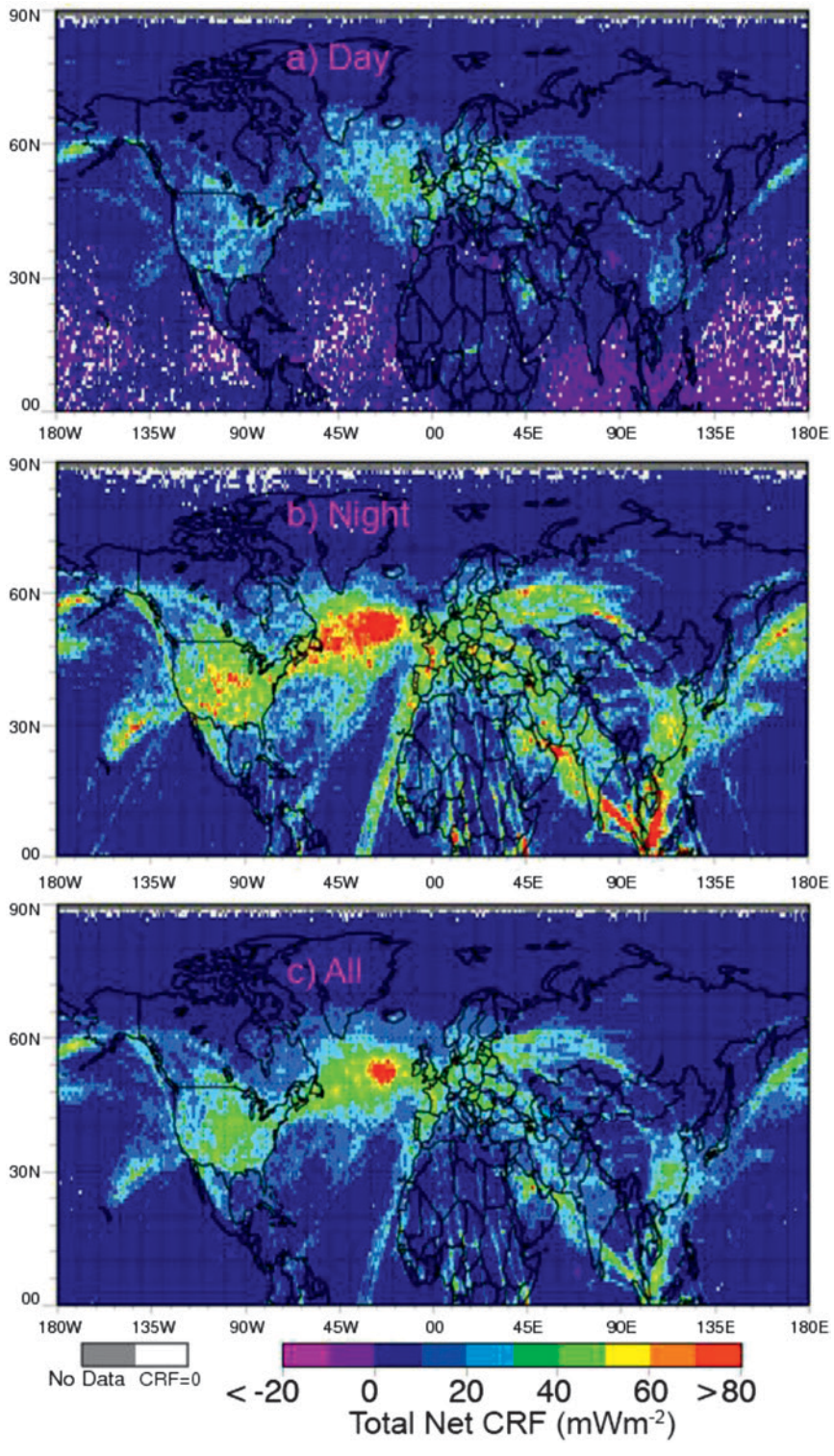

Fig. 5. Mean 2006 net-contrail RF from *Aqua* MODIS data: (a) daytime, (b) nighttime, and (c) all data (NASA Langley).

Using the MODIS results of Duda et al. (2013), Bedka et al. (2013) found an average contrail temperature of −51.8°C with daytime and nighttime modes at −55° and −47°C, respectively, values that are slightly warmer than those from Iwabuchi et al. (2012). Bedka et al. (2013) also retrieved mean COD and D_E values of 0.208 and 34.4 μm, respectively, with a small seasonal cycle in both. The probability distributions of COD from both the *CALIPSO* and MODIS analyses (Fig. 4) are remarkably similar. The mode D_E of 20 μm from the MODIS analysis is also consistent with the *CALIPSO* results. Convergence of these results based on two independent methods greatly increases our confidence in the knowledge of contrail optical properties and subsequent RF computations.

Spangenberg et al. (2013) computed, for the first time, the Northern Hemisphere 2006 LC RF based on simultaneous observations of LCs and associated values of contrail temperature, D_E, and COD from Duda et al. (2013) and Bedka et al. (2013) along with coincident cloud analyses from Minnis et al. (2011) to realistically estimate the background radiation. Figure 5 shows that the greatest net RF (over the North Atlantic) occurs at night (see Fig. 5b) because longwave (LW) and shortwave (SW) forcing cancel each other during the day (see Fig. 5a). Overall, the Northern Hemisphere and global net contrail RFs are 10.6 and 5.7 mW m^{-2}, respectively, for the 2006 *Aqua* results. The global mean net RF is slightly greater than the minimum estimate from Sausen et al. (2005) and is close to the lower end of the RF range, reported by LEE2009 (see Table 5). The previous estimates are based mainly on computations using climate models.

Table 5. Radiative forcings (mW m^{-2}) from models participating in ACCRI, by hemisphere and global average for AEDT 2006 aviation emissions. The minimum and maximum ranges are shown in square brackets where multiple estimates are available. Average and the minimum–maximum range shown are based on ACCRI models that reported hemispheric forcings. Note that not all groups contributed hemispheric RF data and this table does not include the large aerosol indirect effect. Numbers may not add up because of rounding. Aerosol indirect effects are not included because of their large uncertainty, as highlighted by the large differences between participating models. The uncertainties (the minimum and maximum range of evaluations) reported represent the variation between model estimates and are not a comprehensive estimate of uncertainty due to parameter and other uncertainties. Since some groups did not provide data for the table, data from all models are not included.

Forcing agent	NH	SH	NH/SH	Global	LEE2009
CH_4	[−8.0, −12.3]	[−8.0, −12.3]	1	[−8.0, −12.3]	[−2.1, −76.2]
O_3 long	[−4.0, −4.7]	[−4.0, −4.7]	1	[−4.2, −4.5]	—
O_3 short	[10.3, 63.6]	[2.0, 24.1]	[5, 3]	[6.0, 36.5]	[8.4, 82.3]
SO_4 direct	[−5.5, −11.8]	[−0.5, −1.5]	[11, 8]	[−3.0, −7.0]	[−0.79, −29.3]
Nitrate direct	[−11.6]	[−4.2]	[3]	[−4.0, −7.5]	—
BC direct	[1.2, 1.9]	[0.1, 0.2]	[12, 10]	[0.6, 1.0]	[0.56, 20.7]
LCs				[2.9, 11.3]	[5.4, 25.6]
Contrail cirrus	[24.0, 95.0]	[0.7, 5.0]	[34, 19]	[12.4, 51.3]	[12.5, 86.7]

ACCRI CLIMATE MODEL EXPERIMENTS. Using the 2006 air traffic and a temperature-and-humidity-dependent contrail parameterization in CAM5, Chen et al. (2012) found that the simulated contrail coverage is sensitive to model vertical resolution because of assumptions about cloud overlap. With the same model, Chen and Gettelman (2013) estimated the global RF from linear contrails to be equal to 2.9 mW m^{-2}. The RF is nearly half the satellite-based observational estimate (5.7 mW m^{-2}) of linear contrails noted above. The instantaneous RF for contrails is found to exhibit a strong diurnal cycle, as expected (e.g., Meerkötter et al. 1999).

Using CAM5 with a specified linear contrail distribution (Rap et al. 2010), Yi et al. (2012) estimated the 2006 global mean LC net RF to be 11.3 mW m^{-2}. This value was derived by implementing a novel contrail optical property parameterization that is constrained by satellite observations (Xie et al. 2012). The estimated global mean LC net RF is larger than the online simulation result but is slightly lower than the offline simulation result (12.0 mW m^{-2}) by Rap et al. (2010). Global LC net RF is likely overestimated if the natural ice cloud optical property parameterization is used as a proxy for the contrail counterpart in the modeling studies. The regional RF distributions (Fig. 6) reveal that RF in dense air traffic areas (e.g., the United States) is up to 10 times greater than the global average, consistent with observational studies, particularly in the three regions indicated in Fig. 6c, where the RFs are 154.9 (North America), 85.8 (Europe), and 25.0 mW m^{-2} (East Asia). Additional studies for other years are needed to validate these reported high regional magnitudes of RF. Differences in the LC forcing among the models and MODIS observations can mostly be ascribed to differences in the contrail-layer height, D_E; COD model cloud overlap; and other meteorological parameters (Yi et al. 2012), but in general their uncertainty ranges overlap.

Contrail-induced cirrus effects. Because LCs spread to form AICs, the total net AIC RF is likely much larger than the linear contrail forcing. Minnis et al. (2013) tracked selected contrails in satellite observations in otherwise clear skies over the United States and found that the combined linear and contrail cirrus coverage was 3.5 times the LC value, and the contrail cirrus COD and D_E values were greater than the corresponding LC values. If those AIC D_E and COD results are typical, then the RF from Spangenberg et al. (2013) would increase by a factor of ~9, yielding 51.3 mW m^{-2}. However, this estimate based on the MODIS LC analysis may be an upper limit on the AIC RF since the contrails frequently occur with other clouds and are thus not easily identifiable and do not always spread as much as those in the Minnis et al. (2013) study.

CLIMATE MODEL EXPERIMENTS. Chen and Gettelman (2013) assessed the effect of RF due to LC and AIC on global RF. The integrated effect of contrail cirrus, allowing contrails to age to about 30 min is much less sensitive to the diurnal cycle of flights. The global RF

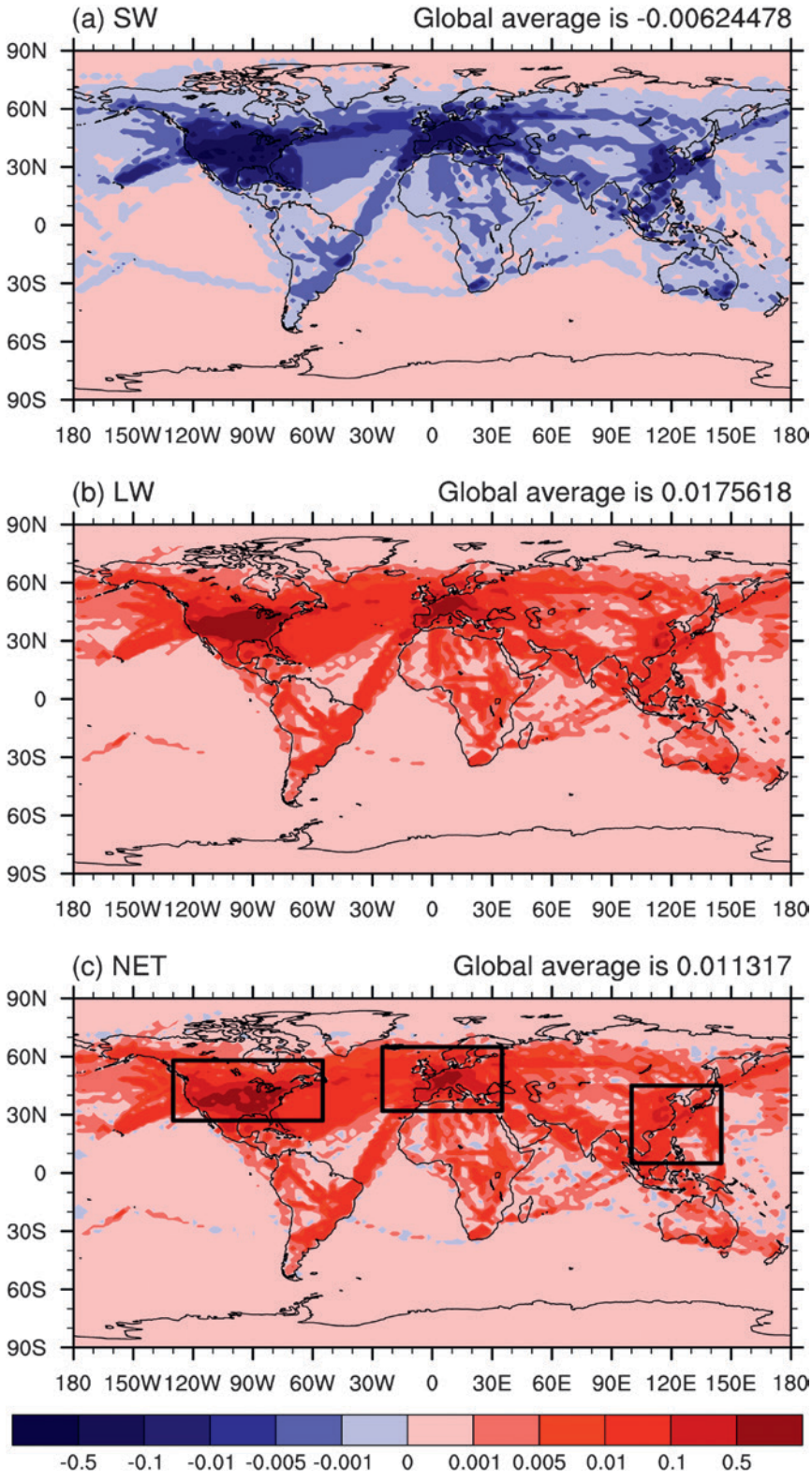

Fig. 6. Simulated 2006 global annual averaged (a) shortwave, (b) longwave, and (c) net linear contrail radiative forcing (W m^{-2}) in the control case. [Adapted from Yi et al. (2012).]

estimate of 4.4–20 mW m^{-2}, with a mean of 12.4 mW m^{-2}, resulting from the spreading of contrails is lower than the "upper bound" estimated from MODIS LC analysis (51 mW m^{-2}) and the AIC-estimated RF of 31 mW m^{-2} by Burkhardt and Kärcher (2011). Over regions with the highest air traffic (central Europe), the local averaged RF can be as large as 1 W m^{-2} (Chen and Gettelman 2013).

Combined observational and modeling studies. Schumann and Graf (2013) found a larger AIC impact using a combination of observations and a contrail cirrus prediction model (CoCiP; Schumann 2012). An "aviation fingerprint" due to a daily cycle of air traffic was found in the diurnal cycle of cirrus properties in the North Atlantic region (NAR) (Graf et al. 2012), which is consistent with the annual mean diurnal cycles of cirrus cover and outgoing LW radiation (OLR) derived from Meteosat data. The NAR fingerprint analysis suggests a contrail cirrus coverage of 1%–2% with optical depths exceeding 0.1 and mean contrail cirrus lifetimes of about 3–4 h over the NAR. Linear contrails contribute a small fraction (<20%) to the contrail cirrus cover at shorter time scales.

The CoCiP model results show an aviation diurnal fingerprint similar to the observations. Hence, contrail cirrus is likely responsible for a large part of the observed effects. The large RF-to-cover ratio suggests that aviation induces additional cirrus cover and thickens existing cirrus. Extrapolation of these

Table 6. Component specific RF (mW m^{-2}) for 2006 emissions as calculated by ACCRI studies.

Study/model used	O_3-S	CH_4	H_2O	SO_4 direct	BC	LC	Contrail cirrus
UIUC CAM5	36.5	−12.3					
GISS-E2	6.0	−8.0	1.3*	−7.0	0.6		
CoCiP							50.0
NASA Langley						5.7	51.3
CAM5				−3.0	1.0	2.9	12.4
Texas A&M						11.3	
IGSM	26.0	−9.7		−4.4			
GEOSCCM	30.5	−12.3	2.0**				

* Includes only change in water vapor due to methane oxidation. Direct emissions of water vapor emissions were not included.
** Represents net RF due to direct emissions of water vapor and change in water vapor due to methane oxidation.

results to the globe using three different models [CAM5, the NASA Langley model, and CoCiP; see Schumann and Graf (2013) and Table 6] implies a global AIC LW RF of 100–160 mW m^{-2}. The corresponding global net RF is determined by estimating the SW RF using the global mean SW/LW RF ratio from models. A ratio of 0.6, used by Schumann and Graf (2013), suggests AIC net RF of about 50 (40–80) mW m^{-2}. If the ratio of 0.4 is adopted (Spangenberg et al. 2013), the net RF would be 50% larger.

Aerosol indirect effects on clouds. Aerosols from aircraft can affect cloud properties by absorbing and scattering solar and thermal–infrared radiation as a result of their direct forcing (see the direct effects of aviation aerosols section above) of climate. They also serve as nucleating sites for cloud drops and ice crystals (see the linear contrails section above) and thereby alter the droplet and crystal numbers in natural clouds. Three ACCRI teams [from the National Center for Atmospheric Research (NCAR), the University of Michigan (UMICH), and Stanford University] investigated these "indirect effects" of aircraft aerosols and found that the largest uncertainties were associated with the impacts of aviation soot on cirrus clouds.

Gettelman and Chen (2013) estimated a very small effect of BC on AIC, while the CAM3+/IMPACT model run at the University of Michigan found that cooling effects ranging from −0.21 to −0.43 W m^{-2} were possible. The indirect effects of aircraft soot on cirrus clouds could be significant, but its quantitative value remains uncertain. Zhou and Penner (2014) found that the forcing by aircraft soot could be as high as 0.8 W m^{-2} if the background atmosphere sulfate numbers that act as freezing nuclei (prior to the addition of aircraft soot) are small or as small as −0.7 W m^{-2} if the background sulfate numbers were higher. IMPACT predicts high background sulfate number concentrations while CAM5 does not, creating differences in their responses to aircraft soot injection. A third model (GATOR-GCMOM) saw net warming due to direct and semidirect effects of soot, especially in the Arctic (Jacobson et al. 2012, 2013).

Gettelman and Chen (2013) using the CAM5 GCM found that sulfate emissions by aircraft at flight altitudes can alter liquid clouds at lower altitudes, thus contributing to shortwave cloud "brightening" through enhanced liquid water path and droplet number, particularly over high-traffic oceans. Globally averaged sulfate direct and indirect effects on liquid clouds of −46 mW m^{-2} were larger than the warming effect of aviation-induced cloudiness (contrail cirrus) of 16 mW m^{-2} (Gettelman and Chen 2013). The net result of including contrail cirrus and aerosols (BC and sulfate indirect effects: 8 and −46 mW m^{-2}, respectively) is a globally averaged cooling of –21 ± 11 mW m^{-2} (Gettelman and Chen 2013). In contrast, the CAM3+/IMPACT model finds no statistically significant effect from aircraft emissions of sulfate on droplet number concentration in liquid clouds.

FUTURE CLIMATE IMPACT PROJECTIONS AND BENEFITS OF MITIGATION SCENARIOS: COMPARISON AGAINST 2006 RESULTS.

While seven models (CAM4, CAM5, IGSM, GISS-E2, GEOSCCM, GATOR-GCMOM, and GEOS-CHEM; see Table 1) simulated climate impacts for 2006, the first five models simulated climate impacts for 2050 scenarios for selected components of aircraft emissions (see Table 4).

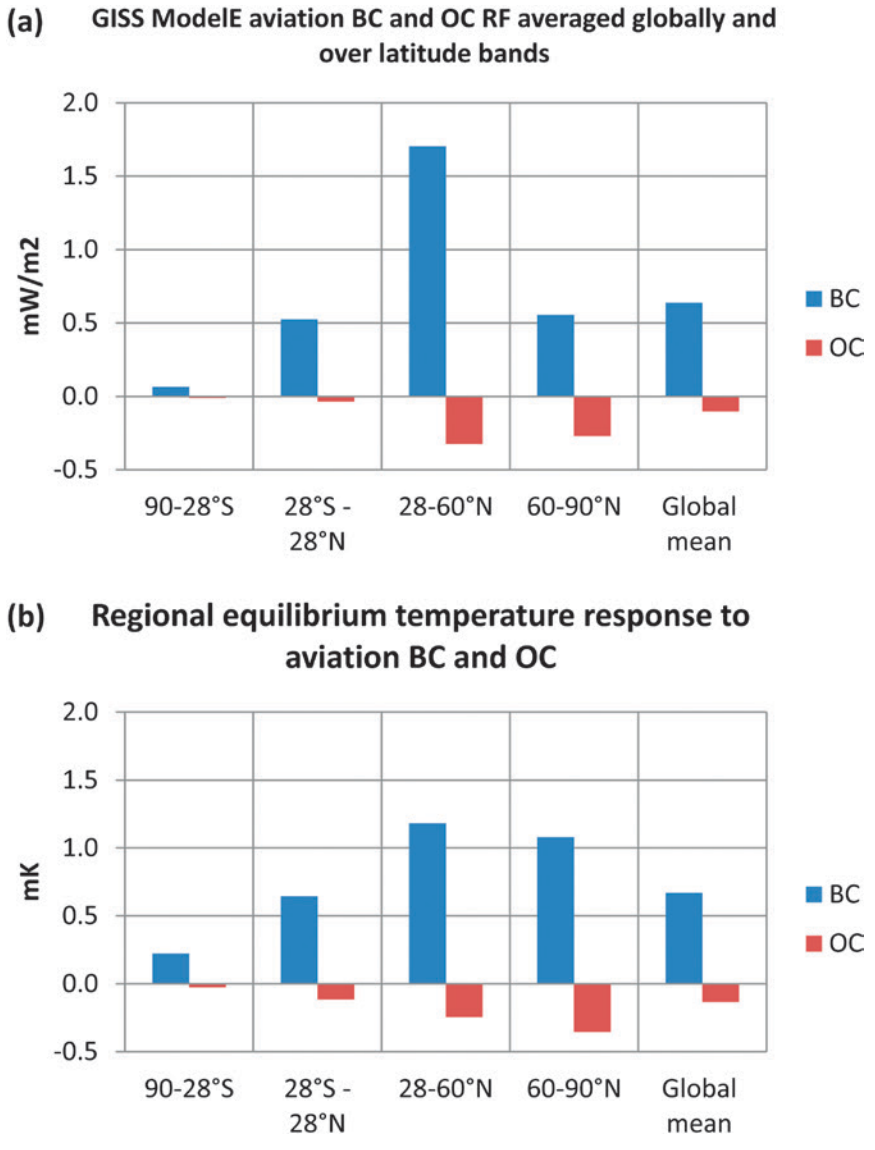

Fig. 7. (a) Radiative forcing of aviation BC and OC aerosols from GISS-E2 averaged globally and over separate latitudinal bands and (b) the corresponding equilibrium surface temperature response estimated using the RTP concept (Shindell and Faluvegi 2010).

Results show that the range of positive RF values for the 2050-baseline case due to changes in short-lived ozone is 30–162 mW m^{-2} whereas the corresponding range for the 2006 case is 6–37 mW m^{-2}. Likewise, the range for a decrease in RF due to changes in methane for the 2050-baseline case is 36–72 mW m^{-2} whereas the corresponding range for 2006 is 8–12 mW m^{-2}. Similar trends (2050 versus 2006) were simulated for changes in RF because of long-term changes in ozone, sulfate, stratospheric water vapor, and BC. Note that for individual models, the directions of the changes in component-specific RF are similar; however, the magnitudes of the changes in RF differ. This is likely due to potential differences in the 2050 background atmosphere simulated by individual models for 2050 and also due to the extent to which these models account for feedback and interactions that are inherent to coupled atmospheric and climate models.

Improvements in aircraft technology and operation procedures (i.e., 2050-S1 scenario) reduced 2050 fuel burn by 43% and aircraft emissions (e.g., 60% for NO_x emissions), which resulted in a significant decrease in simulated RF of individual emissions components. However, the range of these component-specific RF values for the 2050-S1 scenario is still higher than for the corresponding ranges for the 2006 case (see Table 4). For example, the range is 14–71 mW m^{-2} for the change in short-lived ozone for the 2050-S1 scenario whereas the corresponding range for 2006 is 6–37 mW m^{-2}.

Only GISS-E2 and IGSM simulated climate impacts for the 2050-S2 scenario. The RF results for direct impacts of SO_4 and BC aerosols for the 2050-S2 scenario are very low as compared to those for the 2050-baseline and the 2050-S1 scenarios, which is not surprising. Scenario 2050-S2 assumes zero emissions of sulfur and a 50% reduction in BC emissions with the introduction of alternative jet fuels. In particular, the range of direct RF values for sulfate aerosols is from –9 to –2 mW m^{-2} for the 2050-S2 scenario and from –30 to –25 mW m^{-2} for the 2050-Baseline scenario. IGSM reported direct RF results of 0.3 mW m^{-2} for BC, which is a factor of 3 lower than the corresponding value for the 2050-Baseline scenario and is equal to the 2006 value.[4]

[4] The reduction in sulfur emissions in the 2050-S2 scenario does not necessarily take away the cooling benefits of alternative fuels because there could potentially be a corresponding increase in nitrate aerosols, as shown by Unger (2011), and modification to indirect impacts to counteract this decrease in RF.

Scenario 2050-S2 assumed no changes in NO_x emissions. Therefore, very small changes in RF for short-lived ozone and methane were simulated as a result of chemistry interactions. Note that none of the ACCRI models estimated RF for contrails, contrails–cirrus, and indirect RF for the 2050-S2 scenario. We expect that changes in RF for these components could potentially be significantly different because of cloud–aerosol–chemistry–dynamics–radiation interactions and also because of changes in background chemical composition and atmospheric conditions including the cruise-altitude ambient temperature distribution.

REGIONAL CLIMATE IMPACTS. Computations of global mean metrics of climate impacts traditionally use globally averaged input values. In the case of significant spatial variability such as is the case for aviation, global averaging may lead to cancellations

Table 7. Five additional aviation related RF (mWm^{-2}) for 2006 emissions as identified by ACCRI.

Mechanism/ component	2006 RF ($mW\ m^{-2}$) (model)
Long-term ozone	−4.2 (CAM4) and −4.5 (CAM5)
Change in stratospheric water vapor due to change in methane by aviation NO_x emissions	−2.4 (CAM4) and −2.6 (CAM5)
Nitrate aerosol effect	−4.0 (GISS-E2) and −7.5 (IGSM)
Direct and indirect effects of soot aerosols	See text
Direct and indirect effect of sulfate aerosols	See text

METRICS FOR AVIATION EFFECTS ON CLIMATE: ACCRI CONTRIBUTIONS

A key part of ACCRI's focus has been the refinement of analytical tools and metrics that simplify the complex understanding of the science as an aid in decision-making. Typically, metrics aggregate and simplify complex information to a common scale to simplify the comparison of impacts. Metrics such as RF, GWP, RTP, and GTP have proven to be useful tools in climate-policy-related studies. These metrics, especially RF as discussed here, have been reevaluated using ACCRI results both from chemistry–climate models and from observations for contrails.

The RF metric is often used to compare different climate change effects (e.g., IPCC climate assessments), including analyses of the effects of aviation on climate (e.g., Penner et al. 1999; Sausen et al. 2005; LEE2009). The RF concept assumes that at steady state the globally averaged annual mean surface temperature is equal to the globally averaged forcing multiplied by a climate sensitivity factor. Prior to the new findings from ACCRI, the summary analyses for RF in LEE2009 have been held as the standard reference for the understanding of aviation effects on climate. While there remain issues related to its appropriateness as a meaningful metric (Wuebbles et al. 2010), ACCRI studies have updated the values for the globally averaged RFs for individual components. Table 5 shows the RF calculated by different ACCRI studies as a range and compares them with corresponding estimates from LEE2009.

Radiative forcing is a measure of net energy imbalance due to changes in the distribution of radiatively important atmospheric constituents. These distributions and corresponding RF values are affected by the climate as well as atmospheric system feedback and interactions that have been accounted for in modeling simulations. Aviation-related RF values are quite inhomogeneous in space and time and varying degrees of coupling are used by the ACCRI models. Therefore, despite their being a measure of global average values, the component-specific RF values are not linearly added to provide a total RF. This is particularly true when RF values are related to changes in global and regional surface temperature—another important metric for climate response. Only one ACCRI model (GATOR-GCMOM) calculated surface temperature as a climate response of aviation emissions. Additional models are needed to develop and report range results on the climate response of aviation emissions. In addition, the relationship between global and regional RF with surface temperature for non-CO_2 aviation emissions is an area that some in the ACCRI research community are continuing to focus on to quantify the efficacy of the non-CO_2 impacts with respect to CO_2.

In ACCRI, there has been a focus on understanding the linkages between, and interpretations of, different emission metrics, whose key findings are highlighted in D. Wuebbles et al. (2014, unpublished manuscript). In addition to RF this study also considers new ways of presenting metrics for aviation, including the computation and evaluation of GWPs, RTPs, and GTPs with the finding that these values are generally less than 1, much smaller than derived GWPs and GTPs for surface emissions of many important greenhouse gases (e.g., CO_2). An ACCRI-supported study (Peters et al. 2011) provides additional useful insights into the GWP (IPCC 1990, 2007, 2013) and GTP (Shine et al. 2005a,b; IPCC 2013) emissions metrics. The analysis by Peters et al. does not directly use ACCRI results but suggests that the GWP concept does in fact represent a relatively robust, transparent, and policy-relevant emission metric, except for the short-lived climate forcers (e.g., gases with atmospheric lifetimes less than 1 yr) where uncertainties in their interpretation is not known but may be larger (although the GW*p* values are also extremely small for emissions of these compounds).

IMPLEMENTATION OF ACCRI RESULTS IN A SIMPLE CLIMATE MODEL

Simple climate models can be viewed as part of a continuum from simplified metrics to detailed results derived from complex fully coupled chemistry–climate models. The FAA APMT-Impacts (APMT-I) climate module is one such simplified global mean climate model (SCM) that estimates the aviation-attributable burden of climate change in both physical and monetary metrics. The APMT-I climate module adopts the linear impulse response function approach (e.g., Hasselmann et al. 1997; Sausen and Schumann 2000; Shine et al. 2005a,b) to determine the climate response by convoluting the time series of yearly response curves. The aviation climate response is quantified as the difference of impacts due to total anthropogenic emissions and the total less aviation emissions. Effects modeled by the APMT-I climate module include long-lived CO_2, the intermediate-lived impact of NO_x on methane (NO_x–CH_4) and its associated interaction on ozone (NO_x–O_3 long), and the short-lived forcers of NO_x on ozone (NO_x–O_3 short), including the production of aviation-induced cloudiness, sulfates, soot, and H_2O. New short-lived climate forcer (SLCF) pathway, such as the impact of nitrates and the indirect sulfate response identified in ACCRI studies, climate modules are not currently included in the APMT-I and will be added upon their further refinement. The APMT-I climate module accounts for aleatoric and epistemic uncertainties in science, models, valuation, and scenarios along each step of the emissions-to-impact pathway based on the current literature. A detailed description of the modeling approach is provided in Mahashabde et al. (2011), and the most recent model updates and baseline parameter distributions are provided in Wolfe et al. (2014), including the empirical relationship between RF and changes in surface temperature.

The pre-ACCRI APMT-I climate module was evaluated relative to the more complex chemistry–climate models within ACCRI (e.g., Khodayari et al. 2013, 2014), resulting in improvements to APMT. For example, APMT's treatment of oceanic dynamics and carbon cycle processes has been improved. Independently, the new ACCRI uncertainty ranges for SLCFs derived from complex models have been integrated into the APMT-I climate module. Figure SB1 shows the impact of using the range of RF values for four SLCFs (AIC, H_2O vapor, soot, and sulfate aerosols) from ACCRI and for the total aviation on the temperature response compared to pre-ACCRI uncertainty distributions from LEE2009. The reduction in uncertainty results in a 21% decrease in the mean expected maximum temperature response. This change thereby leads to a reduction in the mean net aviation temperature response, which represents the mean of several thousand Monte Carlo runs that sample the entire uncertainty range.

The APMT-I climate module will continue to be updated using the latest scientific understanding beyond ACCRI. As knowledge of the impacts of global aircraft emissions on the hemispheric and regional climate impacts, as well as of indirect components and of future climate impacts—mainly due to contrails and induced cirrus clouds—is advanced, the APMT-I capabilities will be further developed to capture and monetize such impacts for various policy scenarios. Options for the representation of additional metrics (e.g., GTP, RTP, and GWP) in APMT will also be explored. Treatment for the relationship between RF and changes in surface temperature, particularly for short-lived climate forcers, will also be examined.

such that the strength of the regional impacts is obscured (e.g., Shindell and Faluvegi 2010; Shine et al. 2005a,b; Joshi et al. 2011).

There is considerable interhemispheric asymmetry in aviation-induced radiative forcing (Table 5). As expected, the hemispheric (north/south) RF ratios tend to be anticorrelated with the lifetime of the forcing agent—that is, values close to 1 for long-lived species and more than 1 for short-lived species—indicating much higher RF values in the Northern Hemisphere. More discrete correlative analyses of latitudinally and monthly varying aviation component-specific RF values against corresponding fuel burn data are being performed by D. Wuebbles and colleagues.

The spatial distribution of temperature change due to aviation emissions from GATOR-GCMOM also shows regional asymmetry. In this model, aircraft emissions contributed to about 6% (0.15 K) of the observed temperature change in Arctic surface global warming to date (Jacobson et al. 2013). Additional studies are needed to develop confidence in the regional climate impacts of aviation emissions and in the related metrics that properly capture these impacts.

The spatial variability can influence global-mean metrics if there is a nonlinear relationship between the forcing and the response, which is very likely for aviation. Assuming a nonlinear dependence of the climate impact on temperature change, Lund et al. (2012) explored the loss of information about the impacts on smaller spatial scales that result from global metrics in the case of heterogeneous RF caused by short-term climate forcers. As not all ACCRI models simulated the temperature change, the applicability of the Lund et al. (2012) methodology was limited. Instead, the distributions of RFs from ACCRI model simulations have been used in combination with the recently introduced concept of regional temperature change potential (RTP; Shindell and Faluvegi 2009; Shindell 2012) to estimate temperature change in multiple zonal bands. Using GISS-E2 (Unger et al.

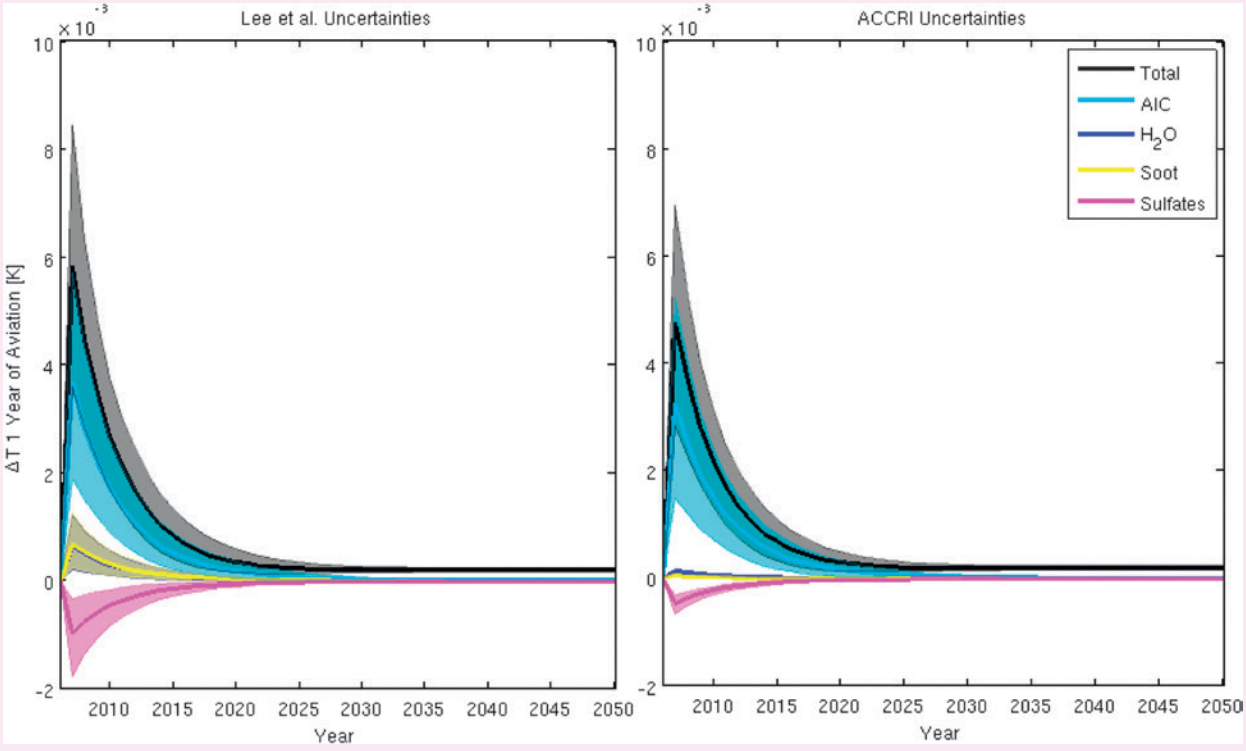

Fig. SB1. Temperature response from 1 yr of aviation emissions. Solid lines represent the best estimates as the ensemble mean.

2013), one can show how RF in adjacent latitude bands contributes to temperature changes in various regions, in addition to the RF exerted within the region (Fig. 7). This illustrates the lack of a one-to-one relationship between the spatial RF pattern and the pattern of the temperature response and indicates how much the regional response (in a given latitude band) deviates from the global-mean level. Further research is currently under way to confirm the applicability of the RTP concept for the aviation sector.

LESSONS LEARNED AND NEXT STEPS. The ACCRI program has made some important contributions to advance the scientific understanding of climate impacts of aviation emissions. While for the first time accounting for nonlinear feedbacks and interactions of the climate system in a comprehensive manner, ACCRI has isolated individual RF contributions and identified a number of new components of aviation RF that have not been considered before (see Table 7). In this study, we have noted that not all models accounted for climate system couplings and feedback processes and computed climate forcing or the response within a single modeling and analysis framework. This limitation prevented us from reporting the mean of the radiative forcing of a given emission component from various models. Therefore, we resorted to reporting the range of values of individual RF components rather than the mean with the associated standard deviation. Similarly, this limitation prevented us from reporting the net radiative forcing due to all aviation emissions combined, which is contrary to previous assessment studies.

Despite the complexities of the climate system, ACCRI helped constrain some uncertainties; however, large uncertainties have emerged in some areas (e.g., indirect effects of aerosols on clouds) that need to be further constrained. Additional studies are needed to develop better estimates of the indirect influences of aviation climate impacts. Atmospheric distributions of volatile sulfate and nitrate aerosols perturbed by

aviation emissions need to be better characterized along with their interplay and role in climate change (and also on surface air quality), particularly given the uncertainty in surface emissions of ammonia and the vertical transport of trace species. Preliminary ACCRI results indicate that deployment of alternative fuels leads to a decrease in climate impacts (e.g., sulfate and BC aerosols). Reduction in these aerosols will also perturb the extent to which they contribute to climate impacts of contrails and induced cirrus clouds. Further studies are warranted to investigate the full range of climate impacts benefits of the uses of alternative jet fuels in relation to conventional fossil-based fuels. Furthermore, changing future atmospheric (ice supersaturation) and climatic (e.g., temperature) conditions at cruise altitude will affect the formation of contrails, as well as cirrus clouds, along with cloud–aerosol interactions. Additional coupled climate studies for future aviation and background emissions scenarios are needed to better quantify the climate impacts of aviation emissions. In particular, the climate impacts of aviation under the different RCP scenarios considered in the IPCC 2014 Assessment Report should be considered in the future.

Aviation emissions are mostly concentrated on flight corridor regions. Therefore, studies are needed to better understand the geographical disparities in regional climate impacts of aviation emissions. Similarly, global average climate impact metrics do not accurately describe regional impacts. Therefore, in addition to properly characterizing regional climate impacts in terms of appropriate metric(s), including transient versus steady-state radiative forcing, a relationship between regional and global climate impacts of aviation emissions also needs to be established. Preliminary post-ACCRI results indicate that individual component-based RF to temperature relationships for non-CO_2 aviation emissions vary significantly, on both global and regional scales. These relationships need to be better defined for their use in simplified climate models. Post-ACCRI activities continue to address some of these important scientific issues.

ACCRI has contributed to the estimation of aviation-induced cirrus cloud climate forcing based on global observation datasets and increased the level of scientific understanding from "very low" to "low." The largest contribution of aviation emissions to climate change results from the presence of contrails and associated cirrus clouds and also from enhanced ozone concentrations in the upper troposphere and lower stratosphere. Some preliminary studies show that an indirect effect of aircraft soot on cirrus clouds could produce a significant cooling, but with a quantitative value that remains highly uncertain.

ACKNOWLEDGMENTS. The ACCRI program at FAA was funded by the Office of Environment and Energy. The DOT's Volpe Center provided assistance in creating and maintaining the aviation emission databases for various scenarios, executing and managing contracts, and conducting annual meetings. We would like to acknowledge critical comments from our colleagues that helped improve this paper.

REFERENCES

Bakan, S., M. Betancour, V. Gayler, and H. Grassl, 1994: Contrail frequency over Europe from NOAA-satellite images. *Ann. Geophys.*, **12**, 962–968, doi:10.1007/s00585-994-0962-y.

Barnes, W. L., T. S. Pagano, and V. V. Salomonson, 1998: Prelaunch characteristics of the Moderate Resolution Imaging Spectroradiometer (MODIS) on EOS-AM1. *IEEE Trans. Geosci. Remote Sens.*, **36**, 1088–1100, doi:10.1109/36.700993.

Barrett, S., and Coauthors, 2010: Guidance on the use of AEDT gridded aircraft emissions in atmospheric models. MIT Laboratory for Aviation and the Environment Rep. LAE-2010-008-N, 13 pp. [Available online at http://lae.mit.edu/uploads/LAE_report_series/2010/LAE-2010-008-N.pdf.]

Bedka, S. T., P. Minnis, D. P. Duda, T. L. Chee, and R. Palikonda, 2013: Properties of linear contrails in the Northern Hemisphere derived from 2006 MODIS observations. *Geophys. Res. Lett.*, **40**, 772–777, doi:10.1029/2012GL054363.

Brasseur, G. P., and M. Gupta, 2010: Impact of aviation on climate: Research priorities. *Bull. Amer. Meteor. Soc.*, **91**, 461–463, doi:10.1175/2009BAMS2850.1.

——, and Coauthors, 1998: European scientific assessment of the atmospheric effects of aircraft emissions. *Atmos. Environ.*, **32**, 2329–2418, doi:10.1016/S1352-2310(97)00486-X.

Burkhardt, U., and B. Kärcher, 2011: Global radiative forcing from contrail cirrus. *Nat. Climate Change*, **1**, 54–58, doi:10.1038/nclimate1068.

——, ——, and U. Schumann, 2010: Global modeling of the contrail and contrail cirrus climate impact. *Bull. Amer. Meteor. Soc.*, **91**, 479–483, doi:10.1175/2009BAMS2656.1.

Busen, R., and U. Schumann, 1995: Visible contrail formation from fuels with different sulfur contents. *Geophys. Res. Lett.*, **22**, 1357–1360, doi:10.1029/95GL01312.

Chen, C.-C., and A. Gettelman, 2013: Simulated radiative forcing from contrails and contrail cirrus. *Atmos. Chem. Phys.*, **13**, 12 525–12 536, doi:10.5194/acpd-13-10939-2013.

——, ——, C. Craig, P. Minnis, and D. P. Duda, 2012: Global contrail coverage simulated by CAM5 with the inventory of 2006 global aircraft emissions. *J. Adv. Model. Earth Syst.*, **4**, M04003, doi:10.1029/2011MS000105.

Duda, D. P., P. Minnis, K. Khlopenkov, T. L. Chee, and R. Boeke, 2013: Estimation of 2006 Northern Hemisphere contrail coverage using MODIS data. *Geophys. Res. Lett.*, **40**, 612–617, doi:10.1002/grl.50097.

EPA–FAA, 2009: Recommended best practice for quantifying speciated organic gas emissions from aircraft equipped with turbofan, turbojet, and turboprop engines, version 1.0. EPA and FAA Rep. EPA-420-R-09-901.

Gettelman, A., and C. C. Chen, 2013: The climate impact of aviation aerosols. *Geophys. Res. Lett.*, **40**, L50520, doi:10.1002/grl.50520.

Graf, K., U. Schumann, H. Mannstein, and B. Mayer, 2012: Aviation induced diurnal North Atlantic cirrus cover cycle. *Geophys. Res. Lett.*, **39**, L16804, doi:10.1029/2012GL052590.

Hasselmann, K., S. Hasselmann, R. Giering, V. Ocana, and H. V. Storch, 1997: Sensitivity study of optimal CO_2 emission paths using a simplified Structural Integrated Assessment Model (SIAM). *Climatic Change*, **37**, 345–386, doi:10.1023/A:1005339625015.

Heymsfield, A., D. Baumgardner, P. Demott, P. Forster, K. Gierens, and B. Karcher, 2010: Contrail microphysics. *Bull. Amer. Meteor. Soc.*, **91**, 465–472, doi:10.1175/2009BAMS2839.1.

Hong, G., and P. Minnis, 2015: Effects of spherical inclusions on scattering properties of small ice cloud particles. *J. Geophys. Res. Atmos.*, **120**, 2951–2969, doi:10.1002/2014JD022494.

ICAO, 2013: *Aviation and Climate Change*. Environment Branch, International Civil Aviation Organization, 207 pp. [Available online at http://cfapp.icao.int/Environmental-Report-2013/index.html#1/z.]

IPCC, 1990: *Scientific Assessment of Climate Change*. Cambridge University Press, 364 pp.

IPCC, 2007: *Climate Change 2007: The Physical Science Basis*. Cambridge University Press, 996 pp.

IPCC, 2013: *Climate Change 2013: The Physical Science Basis*. Cambridge University Press, 1535 pp., doi:10.1017/CBO9781107415324.

Iwabuchi, H., P. Yang, K.-N. Liou, and P. Minnis, 2012: Physical and optical properties of persistent contrails: Climatology and interpretation. *J. Geophys. Res.*, **117**, D06215, doi:10.1029/2011JD017020.

Jacobson, M. Z., J. T. Wilkerson, A. D. Naiman, and S. K. Lele, 2011: The effects of aircraft on climate and pollution. Part I: Numerical methods for treating the subgrid evolution of discrete size- and composition-resolved contrails from all commercial flights worldwide. *J. Comput. Phys.*, **230**, 5115–5132, doi:10.1016/j.jcp.2011.03.031.

——, ——, S. Balasubramanian, W. W. Cooper Jr., and N. Mohleji, 2012: The effects of rerouting aircraft around the Arctic Circle on Arctic and global climate. *Climatic Change*, **115**, 709–724, doi:10.1007/s10584-012-0462-0.

——, ——, A. D. Naiman, and S. K. Lele, 2013: The effects of aircraft on climate and pollution. Part II: 20-year impacts of exhaust from all commercial aircraft worldwide treated individually at the subgrid scale. *Faraday Discuss.*, **165**, 369–382, doi:10.1039/c3fd00034f.

Joshi, M., E. Hawkins, R. Sutton, J. Lowe, and D. Frame, 2011: Projections of when temperature change will exceed 2°C above pre-industrial levels. *Nat. Climate Change*, **1**, 407–412, doi:10.1038/nclimate1261.

Khodayari, A., and Coauthors, 2013: Intercomparison of the capabilities of simplified climate models to project the effects of aviation CO_2 on climate. *Atmos. Environ.*, **75**, 321–328, doi:10.1016/j.atmosenv.2013.03.055.

——, S. C. Olsen, and D. J. Wuebbles, 2014: Evaluation of aviation NO_x-induced radiative forcings for 2005 and 2050. *Atmos. Environ.*, **91**, 95–103, doi:10.1016/j.atmosenv.2014.03.044.

Lee, D. S., D. W. Fahey, P. M. Forster, P. J. Newton, R. C. N. Wit, L. L. Lim, B. Owen, and R. Sausen, 2009: Aviation and global climate change in the 21st century. *Atmos. Environ.*, **43**, 3520–3537, doi:10.1016/j.atmosenv.2009.04.024.

Liou, K. N., Y. Takano, and P. Yang, 2011: Light absorption and scattering by aggregates: Application to black carbon and snow grains. *J. Quant. Spectrosc. Radiat. Transfer*, **112**, 1581–1594, doi:10.1016/j.jqsrt.2011.03.007.

——, ——, Q. Yue, and P. Yang, 2013: On the radiative forcing of contrail cirrus contaminated by black carbon. *Geophys. Res. Lett.*, **40**, 778–784, doi:10.1002/grl.50110.

Lund, M. T., T. Berntsen, J. S. Fuglestvedt, M. Ponater, and K. P. Shine, 2012: How much information is lost by using global-mean climate metrics? An example using the transport sector. *Climatic Change*, **113**, 949–963, doi:10.1007/s10584-011-0391-3.

Mahashabde, A., and Coauthors, 2011: Assessing the environmental impacts of aircraft noise and emissions. *Prog. Aerosp. Sci.*, **47**, 15–52.

Meerkötter, R., U. Schumann, D. R. Doelling, P. Minnis, T. Nakajima, and Y. Tsushima, 1999: Radiative forcing by contrails. *Ann. Geophys.*, **17**, 1080–1094, doi:10.1007/s00585-999-1080-7.

Minnis, P., and Coauthors, 2011: CERES Edition-2 cloud property retrievals using TRMM VIRS and Terra and Aqua MODIS data—Part II: Examples of average results and comparisons with other data. *IEEE Trans. Geosci. Remote Sens.*, **49**, 4401–4430, doi:10.1109/TGRS.2011.2144602.

——, and Coauthors, 2013: Linear contrails and contrail cirrus properties determined from satellite data. *Geophys. Res. Lett.*, **40**, 3220–3226, doi:10.1002/grl.50569.

Naiman, A. D., S. K. Lele, and M. Z. Jacobson, 2011: Large eddy simulations of contrail development: Sensitivity to initial and ambient conditions over first twenty minutes. *J. Geophys. Res.*, **116**, D21208, doi:10.1029/2011JD015806.

Olsen, S. C., D. J. Wuebbles, and B. Owen, 2013a: Comparison of global 3-D aviation emissions datasets. *Atmos. Chem. Phys.*, **13**, 429–441, doi:10.5194/acp-13-429-2013.

——, and Coauthors, 2013b: Comparison of model estimates of the effects of aviation emissions on atmospheric ozone and methane. *Geophys. Res. Lett.*, **40**, 6004–6009, doi:10.1002/2013GL057660.

Oman, L. D., J. R. Ziemke, A. R. Douglass, D. W. Waugh, C. Lang, J. M. Rodriguez, and J. E. Nielsen, 2011: The response of tropical tropospheric ozone to ENSO. *Geophys. Res. Lett.*, **38**, L13706, doi:10.1029/2011GL047865.

Penner, J. E., D. H. Lister, D. J. Griggs, D. J. Dokken, and M. McFarland, Eds., 1999: *Aviation and the Global Atmosphere*. Cambridge University Press, 373 pp.

Peters, G. P., B. Aamaas, T. Bernsten, and J. S. Fuglestvedt, 2011: The integrated global temperature change potential (iGTP) and relationships between emissions metrics. *Environ. Res. Lett.*, **6**, 044021, doi:10.1088/1748-9326/6/4/044021.

Prather, M., R. Sausen, A. S. Grossman, J. M. Haywood, D. Rind, and B. H. Subbaraya, 1999: Potential climate change from aviation. *Aviation and the Global Atmosphere*, J. E. Penner et al., Eds., Cambridge University Press, 185–216.

Prinn, R. G., 2012: Development and application of earth system models. *Proc. Natl. Acad. Sci. USA*, **110** (Suppl. 1), 3673–3680, doi:10.1073/pnas.1107470109.

Rap, A., P. M. Forster, A. Jones, O. Boucher, J. M. Haywood, N. Bellouin, and R. R. De Leon, 2010: Parameterization of contrails in the UK Met Office Climate Model. *J. Geophys. Res.*, **115**, D10205, doi:10.1029/2009JD012443.

Roof, C., and Coauthors, 2007: Aviation Environmental Design Tool (AEDT) system architecture. FAA Rep. AEDT-AD-01.

Sausen, R., and U. Schumann, 2000: Estimates of the climate response to aircraft CO_2 and NO_x emissions scenarios. *Climatic Change*, **44**, 27–58, doi:10.1023/A:1005579306109.

——, and Coauthors, 2005: Aviation radiative forcing in 2000: An update on IPCC (1999). *Meteor. Z.*, **14**, 555–561, doi:10.1127/0941-2948/2005/0049.

Schumann, U., 1994: On the effect of emissions from aircraft engines on the state of the atmosphere. *Ann. Geophys.*, **12**, 365–384, doi:10.1007/s00585-994-0365-0.

——, 1996: On conditions for contrail formation from aircraft exhausts. *Meteor. Z.*, **5**, 4–23.

——, 2012: A contrail cirrus prediction model. *Geosci. Model Dev.*, **5**, 543–580, doi:10.5194/gmd-5-543-2012.

——, and K. Graf, 2013: Aviation-induced cirrus and radiation changes at diurnal timescales. *J. Geophys. Res. Atmos.*, **118**, 2404–2421, doi:10.1002/jgrd.50184.

——, J. Ström, R. Busen, R. Baumann, K. Gierens, M. Krautstrunk, F. Schröder, and J. Stingl, 1996: In situ observations of particles in jet aircraft exhausts and contrails for different sulfur-containing fuels. *J. Geophys. Res.*, **101**, 6853–6869, doi:10.1029/95JD03405.

——, and Coauthors, 2002: Influence of fuel sulfur on the composition of aircraft exhaust plumes: The experiments SULFUR 1-7. *J. Geophys. Res.*, **107**, 4247, doi:10.1029/2001JD000813.

Shindell, D. T., 2012: Evaluation of the absolute regional temperature potential. *Atmos. Chem. Phys.*, **12**, 7955–7960, doi:10.5194/acp-12-7955-2012.

——, and G. Faluvegi, 2009: Climate response to regional radiative forcing during the twentieth century. *Nat. Geosci.*, **2**, 294–300, doi:10.1038/ngeo473.

——, and ——, 2010: The net climate impact of coal-fired power plant emissions. *Atmos. Chem. Phys.*, **10**, 3247–3260, doi:10.5194/acp-10-3247-2010.

Shine, K. P., T. K. Bernstein, J. S. Fuglestvedt, and R. Sausen, 2005a: Scientific issues in the design of metrics for inclusion of oxides of nitrogen in global climate agreements. *Proc. Natl. Acad. Sci. USA*, **102**, 15 768–15 773, doi:10.1073/pnas.0506865102.

——, J. S. Fuglestvedt, K. Hailemariam, and N. Stuber, 2005b: Alternatives to the global warming potential for comparing climate impacts of emissions of greenhouse gases. *Climatic Change*, **68**, 281–302, doi:10.1007/s10584-005-1146-9.

Skowron, A., D. S. Lee, and R. R. De León, 2013: The assessment of the impact of aviation NO_x on ozone and other radiative forcing responses – The importance of representing cruise altitudes accurately. *Atmos. Environ.*, **74**, 159–168, doi:10.1016/j.atmosenv.2013.03.034.

Sokolov, A., and Coauthors, 2009: Probabilistic forecast for twenty-first century climate based on

uncertainties in emissions (without policy) and climate parameters. *J. Climate*, **22**, 5175–5204, doi:10.1175/2009JCLI2863.1.

Spangenberg, D. A., P. Minnis, S. T. Bedka, R. Palikonda, D. P. Duda, and F. G. Rose, 2013: Contrail radiative forcing over the Northern Hemisphere from 2006 Aqua MODIS data. *Geophys. Res. Lett.*, **40**, 595–600, doi:10.1002/grl.50168.

Stevenson, D. S., and Coauthors, 2006: Multimodel ensemble simulations of present-day and near-future tropospheric ozone. *J. Geophys. Res.*, **111**, D08301, doi:10.1029/2005JD006338.

Toohey, D., J. McConnell, L. Avallone, and W. Evans, 2010: Aviation and chemistry and transport processes in the upper troposphere and lower stratosphere. *Bull. Amer. Meteor. Soc.*, **91**, 485–489, doi:10.1175/2009BAMS2841.1.

Unger, N., 2011: Global climate impact of civil aviation for standard and desulfurized jet fuel. *Geophys. Res. Lett.*, **38**, L20803, doi:10.1029/2011GL049289.

——, Y. Zhao, and H. Dang, 2013: Mid-21st century chemical forcing of climate by the civil aviation sector. *Geophys. Res. Lett.*, **40**, 641–645, doi:10.1002/grl.50161.

van Vuuren, D., and Coauthors, 2011: The representative concentration pathways: An overview. *Climatic Change*, **109**, 5–31, doi:10.1007/s10584-011-0148-z.

Wang, M., and J. E. Penner, 2010: Cirrus clouds in a global climate model with a statistical cirrus cloud scheme. *Atmos. Chem. Phys.*, **10**, 5449–5474, doi:10.5194/acp-10-5449-2010.

Wild, O., M. J. Prather, and H. Akimoto, 2001: Indirect long-term global radiative cooling from NO_x emissions. *Geophys. Res. Lett.*, **28**, 1719–1722, doi:10.1029/2000GL012573.

Wilkerson, J. T., M. Z. Jacobson, A. Malwitz, S. Balasubramanian, R. Wayson, G. Fleming, A. D. Naiman, and S. K. Lele, 2010: Analysis of emission data from global commercial aviation: 2004 and 2006. *Atmos. Chem. Phys.*, **10**, 6391–6408, doi:10.5194/acp-10-6391-2010.

Winker, D. M., W. Hunt, and M. J. McGill, 2007: Initial performance assessment of CALIOP. *Geophys. Res. Lett.*, **34**, L19803, doi:10.1029/2007GL030135.

Wolfe, P. J., S. H. Yim, G. Lee, A. Ashok, S. R. H. Barrett, and I. A. Waitz, 2014: Near-airport distribution of the environmental costs of aviation. *Transp. Policy*, **34**, 102–108, doi:10.1016/j.tranpol.2014.02.023.

Wong, H.-W., and R. C. Miake-Lye, 2010: Parametric studies of contrail ice particle formation in jet regime using microphysical parcel modeling. *Atmos. Chem. Phys.*, **10**, 3261, doi:10.5194/acp-10-3261-2010.

——, and Coauthors, 2013: Laboratory and modeling studies on the effects of water and soot emissions and ambient conditions on the properties of contrail ice particles in the jet regime. *Atmos. Chem. Phys.*, **13**, 10 049–10 060, doi:10.5194/acp-13-10049-2013.

Wuebbles, D., M. Gupta, and M. Ko, 2007: Evaluating the impacts of aviation on climate change. *Eos, Trans. Amer. Geophys. Union*, **88**, 157–168, doi:10.1029/2007EO140001.

——, P. Forster, H. Rogers, and R. Herman, 2010: Issues and uncertainties affecting metrics for aviation impacts on climate. *Bull. Amer. Meteor. Soc.*, **91**, 491–496, doi:10.1175/2009BAMS2840.1.

Xie, Y., P. Yang, K.-N. Liou, P. Minnis, and D. P. Duda, 2012: Parameterization of contrail radiative properties for climate studies. *Geophys. Res. Lett.*, **39**, L00F02, doi:10.1029/2012GL054043.

Yang, P., G. Hong, A. E. Dessler, S. C. Ou, K. N. Liou, P. Minnis, and Hashvardhan, 2010: Contrails and induced cirrus: Optics and radiation. *Bull. Amer. Meteor. Soc.*, **91**, 473–478, doi:10.1175/2009BAMS2837.1.

Yi, B., P. Yang, K.-N. Liou, P. Minnis, and J. E. Penner, 2012: Simulation of the global contrail radiative forcing: A sensitivity analysis. *Geophys. Res. Lett.*, **39**, L00F03, doi:10.1029/2012GL054042.

Zhou, C., and J. E. Penner, 2014: Aircraft soot indirect effect on large-scale cirrus clouds: Is the indirect forcing by aircraft soot positive or negative? *J. Geophys. Res. Atmos.*, **119**, 11 303–11 320, doi:10.1002/2014JD021914.